Thermo-mechanical Analysis of Cross ply and Angle ply Laminated Composite Plates

A Dissertation submitted
in partial fulfillment of the requirements
for the degree of

Master of Engineering
in
CAD/CAM Engineering

by

Yadwinder Singh Joshan

Registration No.: 801584021

Under the Supervision of:

Dr. Neeraj Grover

Assistant Professor

Mechanical Engineering Department

MECHANICAL ENGINEERING DEPARTMENT
THAPAR UNIVERSITY, PATIALA

July, 2017

CERTIFICATE

This is to certify that the work done in this thesis report title "**Thermo-mechanical analysis of cross ply and angle ply composite plates**" submitted in partial fulfillment of requirement for the award of Master of Engineering degree in CAD/CAM Engineering in the Mechanical Engineering department of Thapar University, Patiala, is an authentic record of work carried out by me under the guidance of Dr. Neeraj Grover, Mechanical Engineering department, Thapar University, Patiala. The matter embodied in this report has not been submitted in any part or full to any other university or institute for the award of any degree.

Date: 3/7/2017

Yadwinder Singh Joshan

Roll No. 801584021

This is to certify that above declaration made by the student concerned is correct to the best of my knowledge & belief.

Date: 8/7/17

Dr. Neeraj Grover

Assistant Professor, MED

Dedicated to

My Grandfather
Late S. Gurcharan Singh
(1907-2017)

Acknowledgement

I would like to specially acknowledge and extend my heartfelt gratitude to all those who have helped me in completion of this seminar thesis report. With the biggest contribution, I would like to thank Assistant Professor **Dr. Neeraj Grover** sir for his full support and guidance.

Lastly, I would also like to thank my parents for their years of unyielding love and encourage. They have always wanted the best for me and I admire their determination and sacrifice.

Yadwinder Singh Joshan

Abstract

In the present work, the closed form solutions for thermo-mechanical response characteristics of cross-ply and static response characteristics angle-ply plates are developed. The laminated composite plates are modelled in an axiomatic framework based on an inverse hyperbolic shear deformation theory (IHSDT). The principle of virtual work is used to obtain the governing differential equations. The governing differential equations are solved separately for cross-ply and angle-ply plates by consideration of stiffness characteristics of these plates. The sinusoidal and uniform transverse mechanical loading is considered with the linear and non-linear variation of temperature field across the thickness of the plate. The composite plates with simply supported boundary conditions are considered and Navier solutions satisfying the associated boundary constraints are developed. Due to the limitation of applicability of closed form solution only to the simply supported case, the laminated plates are modelled in finite element framework using the potential energy approach. The convergence and accuracy of finite element solution is compared with the closed form solution. The thermo-mechanical response characteristics of cross-ply and static response characteristics angle-ply plates under various boundary conditions are investigated and the results are presented in the non-dimensional form. The obtained results are compared with the existing results for a variety of examples and based on this comparison study, the validity, applicability and accuracy of IHSDT for such analysis is ensured. It is observed from the results that IHSDT can be accurately applied for thermo-mechanical responses of laminated composite plates. The effects of span thickness ratio, boundary conditions, material anisotropy ratio, lamination sequence, loading and thermal conditions, and aspect ratio on the thermo-mechanical response characteristics are also concluded.

Keywords: Laminated composite plates; Thermo-mechanical analysis; Cross-ply and angle-ply plates; Navier solution; Finite element method; Shear deformation theory.

TABLE OF CONTENT

List of Figures

List of Tables

Nomenclature

x, y, z	Cartesian coordinates
u, v	In-plane displacements
$w, \bar{w}$	Dimensional and non-dimensional transverse deflection
u_0, v_0, w_0	Mid-plane displacements
a, b, h	Length, breadth and thickness of the plate
T	Temperature
$\left[\bar{Q}_{ij}\right]^{(k)}$	Transformed reduced stiffness matrix
E	Elasticity coefficient
G	Rigidity coefficient
ν	Poisons ratio
U	Strain energy
W	Work done by the applied force
$\{F\}$	Force vector
N, M, P	In-plane stress, moment and higher order moment resultants
S, K	Transverse shear stress and moment resultants
R	Resultant stiffness matrix
q	Transverse load

Greek Symbols

θ	Angle of fiber orientation
θ_x, θ_y	Shear rotations
$\varepsilon_{xx}, \varepsilon_{yy}$	In-plane normal strains
γ_{xy}	In-plane shear strain
γ_{xz}, γ_{yz}	Transverse shear strains
$\left\{\varepsilon^{Th}\right\}$	Thermal strain vector
α	Coefficient of thermal expansion
$\sigma, \bar{\sigma}$	Dimensional and non-dimensional normal stress
τ	Shear stress
Δ	Generalised displacement vector

Acronyms

CFS	Closed form solution
CLPT	Classical laminated plate theory
ESL	Equivalent single layer
FEM	Finite Element method
FSDT	First order shear deformation theory
HSDT	Higher order shear deformation theory
IHSDT	Inverse hyperbolic shear deformation theory
SPT	Sinusoidal plate theory
SSL	Sinusoidal load
UDL	Uniformly distributed load

CHAPTER-1 INTRODUCTION

1.1. Composite materials

Macroscopically combined two and more different kind of materials yield to form a new material known as composite material. The composite material is composed of two distinct phases, continuous phase and non- continuous phase. These distinct phases are physically and chemically different from each other. The supporting phase is known as matrix and the strengthening phase is known as reinforcement as illustrated in Fig.1.1.

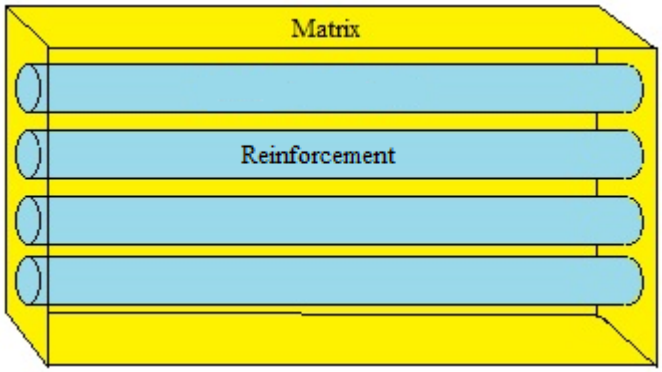

Figure 1.1: Matrix and Reinforcement

Matrix is the supporting and binding phase to hold the reinforcement together. Matrix supports the structure of the reinforcement and the mechanical properties like shear properties, compression properties and stiffness modulus are influenced by the matrix materials. Matrix transfers the loads and stresses acting on the composite to the reinforcement.

Reinforcement is the discontinuous phase in composites and provide strength to the structure. The reinforcement may be in the form of fibre, particles or whiskers. Reinforcement provides strength and stiffness to composites. On the basis of types of reinforcement present in composite, the composites can be classified in two types:-

1. Particulate reinforced composites

2. Fibrous reinforced composites

1. **Particulate reinforced composites** have one or more types of material particles as reinforcement bounded together by matrix. The reinforcement present in these composites

may be in dispersed phase as in carbon nano tubes reinforced composites. The particles in the composites can be randomly oriented or may in preferred manner.

2. **Fibrous reinforced composites** have fibers as reinforcing materials bounded by matrix. Fibers are the vital class of reinforcements, as fibers give strength to the continuous phase increasing the mechanical properties as needed.

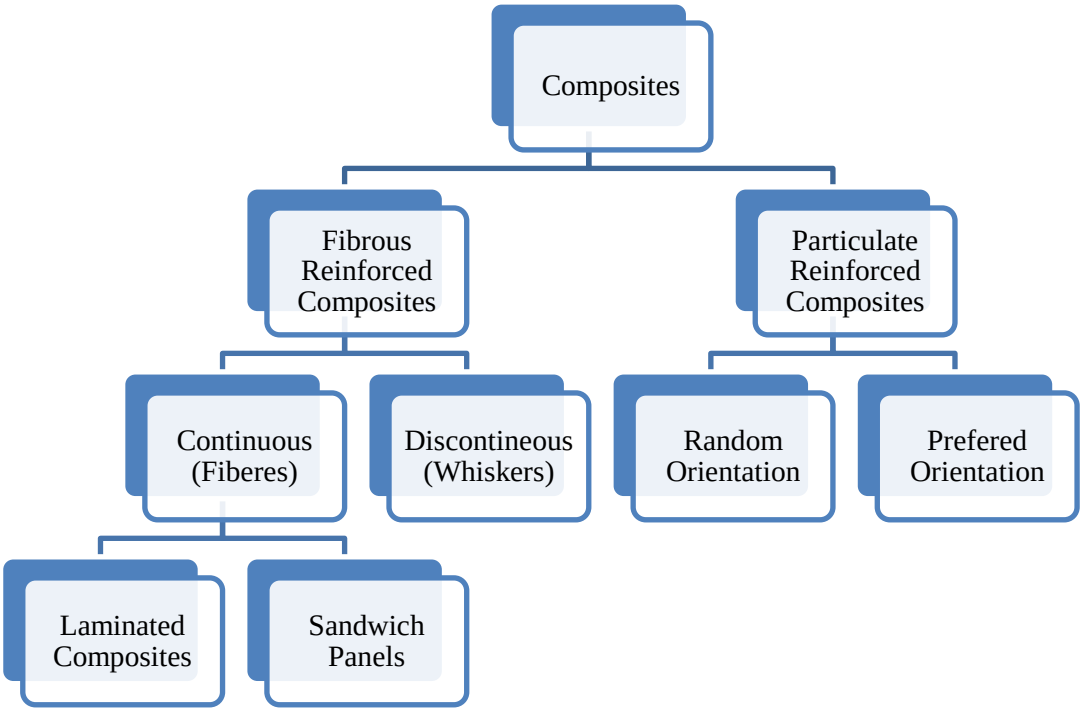

Figure 1.2: Classification of composites on the basis of type of reinforcement

The reinforcing fibers con be continuous in the matrix or can be discontinuous. These discontinuous fibers are known as whiskers. Fibrous reinforced composites are stacked together to form multi-layered composites. The stiffness characteristics of each layer of composites is dependent on the angle of orientation of the fiber. The multi-layered composites are designed as desired by varying the fiber orientation of each layer. These multilayered composites having each layer of equal thickness are known as laminated composites. In order to increase the bending stiffness of multi-layered composites the low density centre layer of the composite known as core is stacked in the multilayered composites, There types of composites are known as sandwich panels as illustrated in Fig. 1.3.

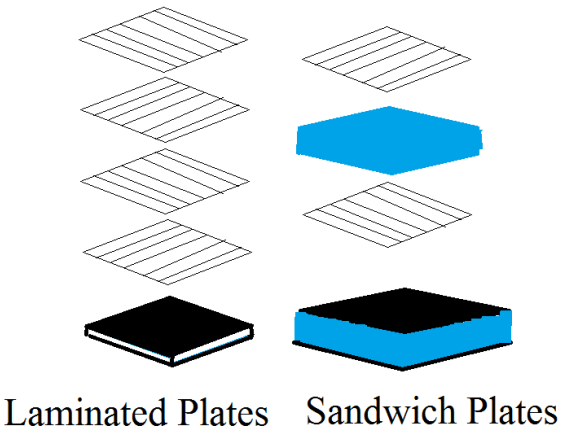

Figure 1.3: Laminated and Sandwich Plates

1.2. Advantages of composites

The various properties that enhances the use of composites in structures and other applications are enlisted as under:

1. Better specific strength
2. Better fatigue resistance.
3. Higher specific stiffness
4. Impact resistance
5. Design flexibility
6. Chemical Resistance

1.3. Applications of composites

1. Automotive Industry
2. Aerospace industry

There is wide application of these advanced materials in many engineering applications such as marine structures, sports equipments, railway coaches, nuclear power plants, etc.

In most of the applications, the composite structures are influenced by the thermal gradient, as in aerospace and marine applications. Moreover, the temperature field is variable across the thickness. As in aerospace, the temperature is different inside the cabin for comfort of the

passengers and outside temperature is dependent on environmental conditions and elevation. The temperature variations tends to deform the structure. Therefore, it becomes necessary to analyse the composite structures under thermo-mechanical loading. The analysis of multilayered composites is challenging due to their anisotropic nature. The elasticity and thermal expansion coefficients of multilayered composites are different in different directions and also vary along the thickness due to change of fiber orientation in the different layers.

1.4. Summery

The increased use of composites at elevated temperature environment have encouraged the researchers to predict the behaviour of composites under the thermal loading in order to optimize the usage of composites and ensure a superior design.

CHAPTER-2 LITERATURE REVIEW

2.1. Introduction

The composite structures have been investigated through many approaches in the past. The complicating effects of these composite structures have been addressed in a variety of ways. One such requirement is the existence of shear deformation effects in the composite materials. A number of theories have been developed during last three decades. In the displacement based axiomatic framework of laminated composite plates, the development of theories is observed in the equivalent single layer (ESL) approach, layer wise (LW) approach, and zig zag (zz) approach. In the framework of ESL theories, the development is mainly focused on the shear deformation and accurately predicting the response of the multilayered structures.

2.2. Modelling of composite plates

The composite structures have been investigated through many approaches in the past. The complicating effects of these composite structures have been addressed in a variety of ways. The researchers have modelled the composite plates in many ways described as under:-

Love (1927) presented the theory of elasticity for plates. This theory considered that the plate having single layer. The assumption was made that the normal to the plane before application of load remains normal after the application of load. Only the in-plane stresses were considered. The thickness of the plate remains same after deformation. The effect of transverse shear stresses was neglected.

Koiter (1960) implemented the theory of elasticity on thin shells. It was based on the energy considerations. It was recommended that the in-plane as well as transverse shear stresses should be taken into account.

Reissner and Stavwsky (1961) applied mathematical theory of elasticity presented by Love (1927) on multilayered structures later referred to as classical laminated plate theory (CLPT). The geometrical interpretation of this model is shown in Fig. 2.1.

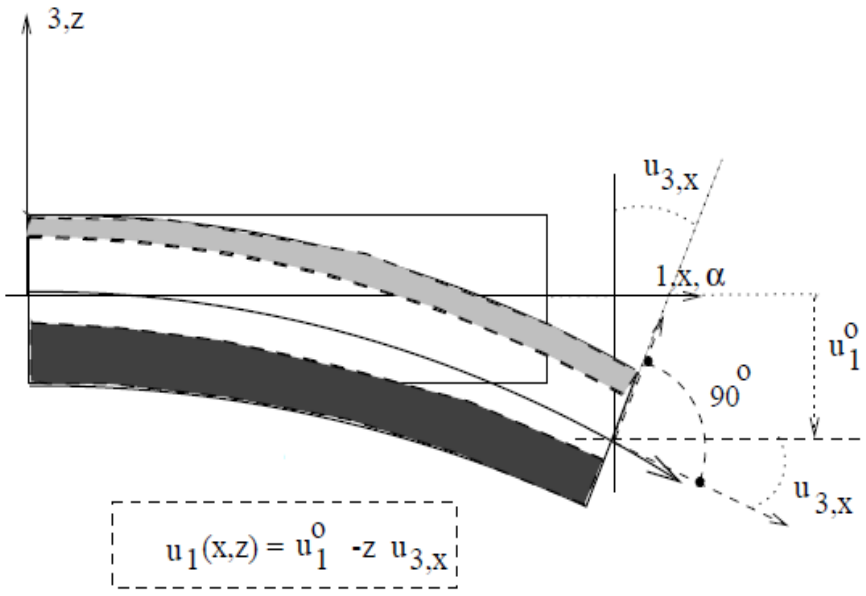

Figure 2.1: CLPT Displacement Model [Carrera, 2002]

The assumptions that were assumed by Love were also considered in this model. Also the effect of transverse shear stresses were again neglected in this model.

Reissner (1945) and Mindlin (1951) examined the effects of transverse shear deformation of the plates on static response extended in the form of first order shear deformation theory (FSDT). The displacement kinematics in terms of mid plane displacements (u_0, v_0, w_0) of FSDT is as follows:

$$u = u_0 + z\phi$$
$$v = v_0 + z\phi$$
$$w = w_0$$

The parameters *u*, *v* and *w* denote the at any point of the plate in cartesian coordinates. The term φ is the rotation between the two normal's as shown in Fig. 2.2. The assumptions made in CLPT were refined in FSDT. However, the value of transverse shear stresses were not obtained equal to zero at top and bottom of the plate described in Fig. 2.3. The transverse shear stresses were obtained constant along the thickness of the plate and the discontinuity was observed at the layer interface. The discontinuity in the value of transverse shear stresses can be clearly observed in Fig. 2.3.

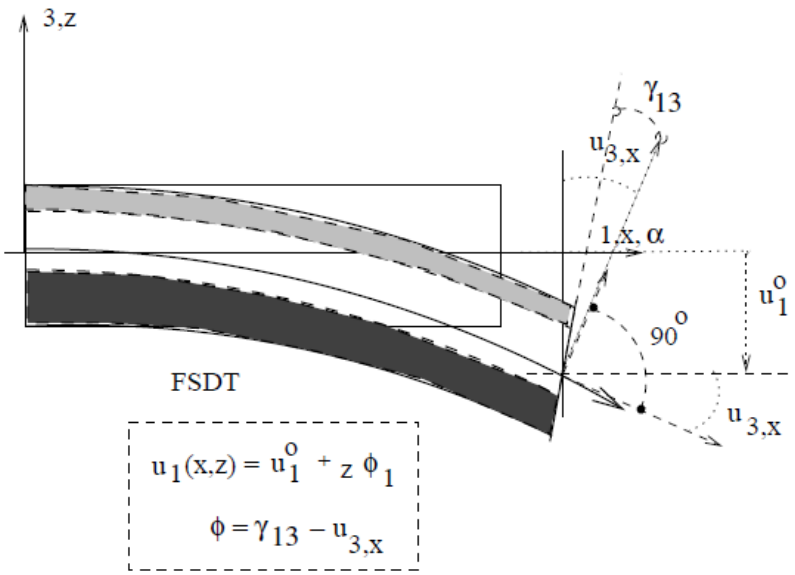

Figure 2.2: FSDT Displacement Model [Carrera, 2002]

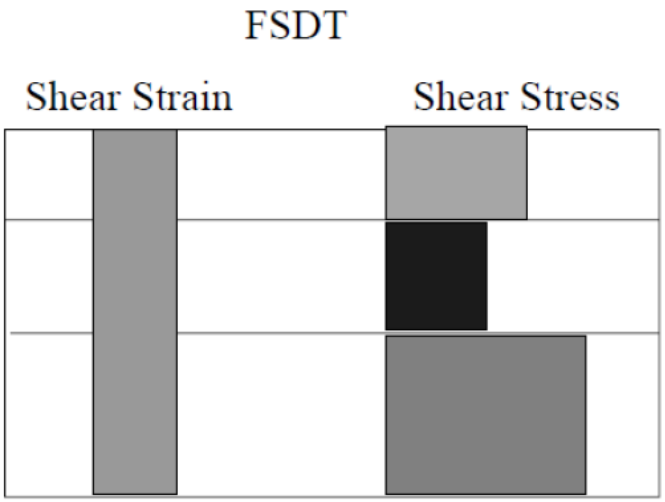

Figure 2.3: Shear stresses and strains in FSDT [Carrera, 2002]

Hence, later on there was the use of correction factor in FSDT that increased the complexities as it was dependent on various parameters which lead to extension of FSDT to higher order shear deformation theories which are classified into two types:-

1. Polynomial Shear Deformation Theories
2. Non- Polynomial Shear Deformation Theories.

2.3. Polynomial shear deformation theories

In polynomial shear deformation theories (PSDTs), the displacement field is expressed in terms of thickness coordinates using Taylor series expansion. The higher order terms of thickness coordinate expressed in terms of coefficients of shear rotations in the displacement field.

Reddy (1984) presented first Higher order shear deformation theory(HSDT) which was the refinement in the FSDT. A higher order term of thickness coordinate was added along with displacement field of FSDT and the shear stresses and strains were executed to as zero on top and bottom surface as shown in Fig. 2.4. The theory gave approx. 93% correct results for displacement and stresses as compared to the three-dimensional closed form solution.

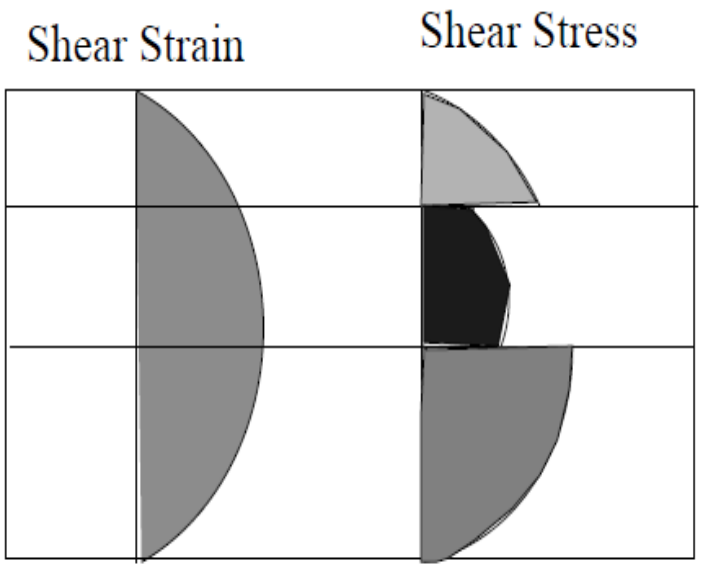

Figure 2.4: Shear stresses and strains in HSDT [Carrera, 2002]

Kant and Pandya (1988) presented a new refined polynomial shear deformation theory for the study of vibrations on laminated composite plates. the well known principles of Hamilton's was used to develop governing equations.

Maiti and Sinha (1994) analysed the response of bending and vibrations on laminated composite plates using and 8 nodded element both for FSDT and HSDT .Both the cross-ply and angle ply laminated plate were analysed.

Swaminathan and Paul (2007) analysed angle-ply laminated plates under static load using a polynomial higher order theory having twelve parameters in the displacement field. Due to large number of degrees of freedom considered in the displacement field, this theory was computationally expressive as compared to other PSDTs.

2.4. Non-polynomial shear deformation theories

Non-polynomial shear deformation theories (NPSDTs) have a non-polynomial function of the thickness coordinate in the displacement field. These non-polynomial functions are optimized in order to obtain the accurate results.

Aydogdu (2008) presented a non polynomial shear deformation theory using an exponential function of thickness co-ordinate. Bending and stress analysis under transverse load, free vibration and buckling for cross ply simply supported composite plates were analysed using the analytical solution.

Mieche et al. (2011) presented shear deformation theory based on a hyoerbolic function of thickness coordinate for buckling and free vibration analysis of functionally graded (FG) plates. The principle of virtual work was implemented in order to derive the governing equations.

Mantari et al. (2011) presented a theory for both laminated an sandwich composite plates and shells for static and dynamic analysis using a trigonometric function.

Grover et al. (2013) presented inverse hyperbolic shear deformation theory (IHSDT). This theory was employed for static and buckling analysis of laminated and sandwich, square and rectangular plates.

- Accuracy level 97% for static analysis.
- No use of shear correction factor.
- Better results for thick plates.
- Same number of parameter involved as that of FSDT.

The percentage errors are calculated from the tabulated results given by Grover et al.(2013), Reddy (1984), Mantari (2011), and Karama (2009) are illustrated in Fig. 2.5. It is observed

that the error corresponding to IHSDT is less as compared to others for the considered structural analysis.

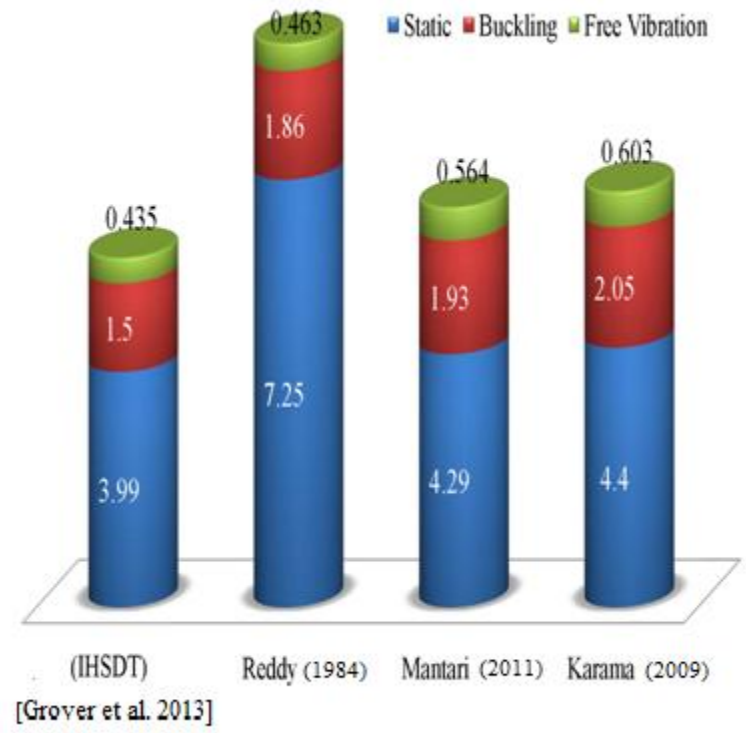

Figure 2.5: Percentage error of various theories from exact solution for various structural responses.

Thai et al. (2014) presented an inverse trigonometric shear deformable theory for cross ply static, buckling and free vibration response of multilayered and sandwich composite plates. the solution was obtained using finite element model for simply supported rectangular plates and elliptical shells.

Carrera (2002) presented an extenssive review paper on the theories used for analysis of laminated plates and shells. This paper included the basic of the theories (including CLPT, FSDT and PHSDT), assumptions assumed by the theory and the limitations.

2.5. Thermo-mechanical analysis of composite plates

Thermo-Mechanical analysis of composite plates refer to the analysis under the combined effect of mechanical loading and temperature. The temperature field may be constant, or may be varying uniformly and non-linearly along the transverse direction of the plate .The

analysis of composite structures under the thermal environment have been investigated by various researchers using various displacement based theories.

Wu and Tauchert (1980) investigated the behaviour of simply supported anti symmetric cross-ply and angle-ply rectangular laminates using classical laminated plate theory (CLPT) under constant and linearly varying temperature. The assumptions of CLPT were taken into account as the effect of transverse shear stresses was neglected. An analytical solution both for cross-ply and angle-ply plates using Navier's solution are employed.

Reddy and Hsu (1980) presented the closed form solution for the cross-ply laminated plates under thermal bending and used finite element formulation to illustrate results for angle-ply laminates using FSDT. The effect of change in the material properties, aspect ratio, lamination sequence and loading conditions on non dimensional transverse deflection under linearly varying temperature field were illustrated.

Khdeir and Reddy (1991) implemented Levy solution to investigate thermo static analysis of cross-ply composite plate under various boundary conditions using CLPT, FSDT and HSDT. Levy solution is an analytical solution applicable to various boundary conditions of the laminated plate.

The finite element model for non-linear static and dynamic analysis of laminated plates under thermal loading was developed by Chandrashekhara K. and Tenneti R. (1994).

Bhaskar et al. (1996) investigated thermo-elastic behaviour of laminated plates and strips using the equilibrium conditions. The three dimensional results for cross-ply strips were also illustrated.

Fares and Zenkour (1999) illustrated thermal bending of laminated composite plates using mixed variational formula. The refinement in the displacement field of FSDT was made for thermo-mechanical analysis of laminated plates.

Khare et al. (2003) investigated simply supported laminated cross-ply curved shells implementing HSDT under thermal gradient using a closed form solution. the results were presented for mainly cylindrical shells.

Zenkour (2004) presented Navier type closed form solution for analysis of cross-ply laminated plates using sinusoidal plate theory (SPT). The cross-ply plates were analysed under linearly and non-linearly varying thermal loading.

Mechab et al. (2012) studied thick orthotropic and cross-ply plates under thermal gradient using various higher order theories including HSDT and SPT using an analytical solution.

Cetkovic M. (2015) studied the thermo mechanical behaviour of laminated and sandwich plates using layer-wise approach. The layer-wise approach is computationally expensive as compared to ESL approach, as it considers different parameters for different layers.

2.6. Observations from literature

The literature available in the context of modelling of composite plates and thermo-mechanical analysis of cross-ply and angle-ply laminated composite plates are reviewed and following observations are made :

1. The analytical solution for static analysis of angle-ply plates for non-polynomial shear deformation theories are not available.
2. The analytical solution for thermo-mechanical analysis of cross-ply for IHSDT are not available.
3. The analytical solution for thermo-mechanical analysis of angle-ply plates for higher order shear deformation theories not available.
4. The numerical solutions for thermo-mechanical analysis of cross-ply plates for non-polynomial shear deformation theories are not available.
5. The numerical solutions for thermo-mechanical analysis of angle-ply plates for non-polynomial shear deformation theories are not available.

On the basis of these observations from the literature the objectives and scope of the present work are as follows:

2.7. Objective of the present work

The objective of the present work is to examine the thermo-mechanical response characteristics of cross ply and angle ply laminated composite plates in analytical and finite element framework.

2.8. Scope of the present work

1. Analytical modelling of cross ply plates for thermo-mechanical analysis.
2. Analytical modelling of angle-ply plates for static analysis
3. Analytical modelling of angle ply plates for thermo-mechanical analysis.
4. Finite Element Modelling of cross ply and angle ply plates for thermo-mechanical analysis.

2.9. Summery

The articles available in the literature in the context of thermo-mechanical analysis of multilayered plates are studied and various observations are made on the bass of the literature review. On the basis of observations made from the literature the objectives are set for the present research work.

CHAPTER-3 MATHEMATICAL FORMULATION

3.1. Introduction

In this section, the composite plates are modelled analytically in the axiomatic framework using inverse hyperbolic shear deformation theory (IHSDT). The governing differential equations are yielded by implementing the principle of virtual work. These governing equations are solved separately for cross-ply and angle-ply plates by consideration of stiffness characteristics of these plates. The sinusoidal and uniform transverse mechanical loading is considered with the linear and non-linear distribution of temperature across the depth of the plate. The simply supported composite plates are considered and Navier solutions satisfying the associated boundary constraints are developed for both cross-ply and angle-ply plates.

A fiber-reinforced laminated composite plate having length *a*, breadth *b* and overall thickness as *h* subjected to a static transverse load $q(x, y)$ and a temperature field $T(x, y, z)$ is considered in the present work. The plate consists of *n* number of equal thickness layers stacked together to form the laminated plate. The schematic of the laminated composite plate in the Cartesian co-ordinate system is shown Fig. 3.1.

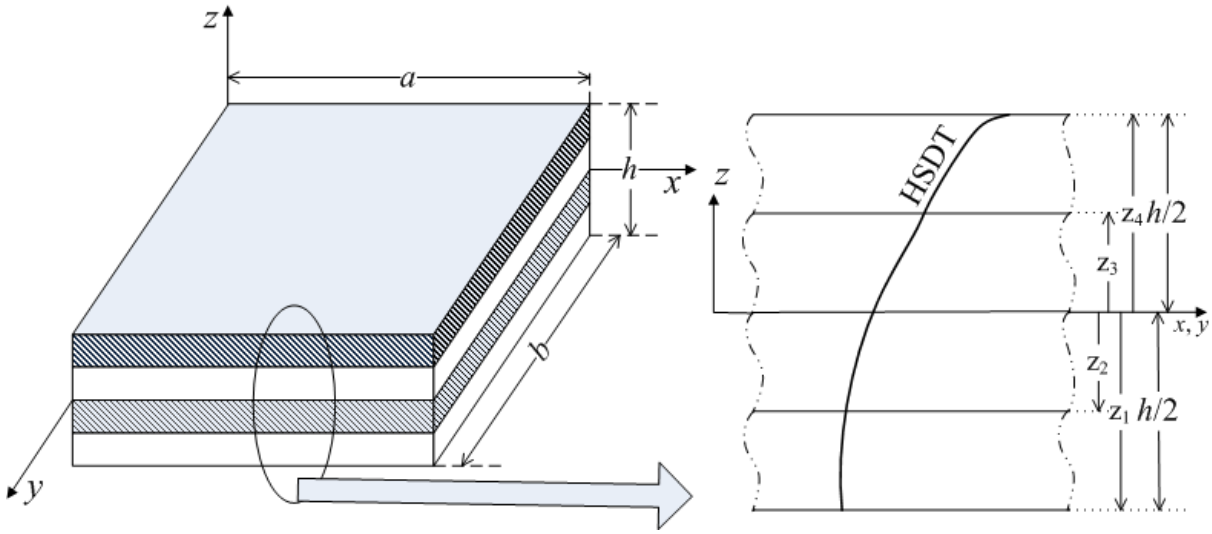

Figure 3.1: Laminate geometry and co-ordinate system

3.2. Displacement and temperature field

The present formulation is based on the axiomatic formulation in which the displacements are primary variables. The in-plane displacements (u, v) and transverse displacement (w), at any

point (*x, y, z*) in the laminated composite plate are expressed in the framework of an inverse hyperbolic shear deformation theory (IHSDT) [Grover et al. 2013].

$$\begin{aligned} u(x,y,z) &= u_0(x,y) - z\frac{\partial w_0}{\partial x} + f(z)\theta_x \\ v(x,y,z) &= v_0(x,y) - z\frac{\partial w_0}{\partial y} + f(z)\theta_y \\ w(x,y,z) &= w_0(x,y) \end{aligned} \tag{2.1}$$

where u_0 , v_0 are the in-plane deformations of the middle surface along *x* and *y* co-ordinates respectively and w_0 is the transverse deformation of the middle surface. The parameters θ_x and θ_y are the shear rotations. The function *f(z)* is taken such that

$$\begin{aligned} f(z) &= g(z) + \Omega z \\ g(z) &= \sinh^{-1}\left(\frac{rz}{h}\right) \\ \Omega &= \frac{2r}{h\sqrt{r^2+4}} \end{aligned} \tag{3.2}$$

where *g(z)* is the inverse hyperbolic function of *z* and Ω is a constant for a laminated plate having a thickness *h.* The parameter *r* is chosen in order to optimize the results with respect to three dimensional theory and its value is chosen as 3. The value of Ω is taken in such a way that the values of transverse shear strains at the top and bottom of the laminated composite plate tend to zero thereby facilitating the satisfaction of transverse shear conditions at top and bottom and hence eliminating the requirement of shear correction factor. The applied temperature is distributed across the thickness and the temperature distribution is assumed to be consistent with the present inverse hyperbolic shear deformation theory.

$$T(x,y,z) = T_1(x,y) + \frac{z}{h}T_2(x,y) + \frac{f(z)}{h}T_3(x,y) \tag{3.3}$$

where T_1, T_2 and T_3 represents constant, linearly varying and non-linearly varying temperature field respectively.

3.3. Strain displacement relations

The laminated composite plates are considered to be constituted of the composite material which undergoes linear deformation. Therefore, linear strain-displacement relations as indicated in Eq. (2.4) are implemented for depicting the structural kinematics.

$$
\begin{aligned}
\varepsilon_{\mathrm{xx}} &= \frac{\partial u}{\partial x} = \frac{\partial u_0}{\partial x} - z\frac{\partial^2 w_0}{\partial x^2} + f(z)\frac{\partial \theta_x}{\partial x} \\
\varepsilon_{\mathrm{yy}} &= \frac{\partial v}{\partial y} = \frac{\partial v_0}{\partial y} - z\frac{\partial^2 w_0}{\partial y^2} + f(z)\frac{\partial \theta_y}{\partial y} \\
\gamma_{\mathrm{xy}} &= \frac{\partial u}{\partial y} + \frac{\partial v}{\partial x} = \frac{\partial u_0}{\partial y} + \frac{\partial v_0}{\partial x} - z\frac{2\partial^2 w_0}{\partial x \partial y} + f(z)\left(\frac{\partial \theta_x}{\partial y} + \frac{\partial \theta_y}{\partial x}\right) \\
\gamma_{\mathrm{yz}} &= \frac{\partial v}{\partial z} + \frac{\partial w}{\partial y} = f'(z)\theta_y \\
\gamma_{\mathrm{xz}} &= \frac{\partial u}{\partial z} + \frac{\partial w}{\partial x} = f'(z)\theta_x
\end{aligned}
\tag{2.4}
$$

The parameters $\varepsilon_{\mathrm{xx}}$ and $\varepsilon_{\mathrm{yy}}$ are normal strains in *x* and *y* direction respectively, γ_{xy} is the in-plane shear strain while γ_{xz} and γ_{yz} are the transverse shear strains. It is clearly observable from the Eq. (2.4) that transverse shear strains (γ_{xz} and γ_{yz}) are dependent on respective shear rotations and $f'(z)$ where prime (') in $f'(z)$ denotes derivative of function $f(z)$ with respect to *z*. This clarifies the direct dependence of transverse shear strains on $f'(z)$.

3.4. Stress strain relations

The material behaviour of the composites is depicted with the help of constitutive relation for the individual layers. The stress components $\{\sigma\} = \begin{bmatrix} \sigma_{xx} & \sigma_{yy} & \tau_{xy} & \tau_{yz} & \tau_{zx} \end{bmatrix}^T$ for a general k^{th} layer are related to strain components $\{\varepsilon\}$ and temperature induced strains $\{\varepsilon^{Th}\}$ in the following manner:

$$
\begin{Bmatrix} \sigma_{xx} \\ \sigma_{yy} \\ \tau_{xy} \\ \tau_{yz} \\ \tau_{xz} \end{Bmatrix}^{(k)} = \begin{bmatrix} \bar{Q}_{11} & \bar{Q}_{12} & \bar{Q}_{16} & 0 & 0 \\ \bar{Q}_{12} & \bar{Q}_{22} & \bar{Q}_{26} & 0 & 0 \\ \bar{Q}_{16} & \bar{Q}_{26} & \bar{Q}_{66} & 0 & 0 \\ 0 & 0 & 0 & \bar{Q}_{44} & \bar{Q}_{45} \\ 0 & 0 & 0 & \bar{Q}_{45} & \bar{Q}_{55} \end{bmatrix}^{(k)} \left(\begin{Bmatrix} \varepsilon_{xx} \\ \varepsilon_{yy} \\ \gamma_{xy} \\ \gamma_{yz} \\ \gamma_{xz} \end{Bmatrix}^{(k)} - \begin{Bmatrix} \alpha_{xx} \\ \alpha_{yy} \\ \alpha_{xy} \\ 0 \\ 0 \end{Bmatrix}^{(k)} T \right)
\tag{3.5}
$$

or

$$
\{\sigma\}^{(k)} = \left[\bar{Q}_{ij}\right]^{(k)} \left(\{\varepsilon\}^{(k)} - \{\varepsilon^{Th}\}^{(k)} \right)
$$

The matrix $\left[\overline{Q}_{ij}\right]^{(k)}$ represents the reduced transformed stiffness matrix for the k^{th} layer which is a function of reduced stiffness matrix $\left[Q_{ij}\right]$ and fiber orientation (Θ) while the reduced stiffness matrix is expressed in the terms of orthotropic material properties (E_{11}, E_{22}, G_{12}, G_{23}, G_{13}, ν_{12}, ν_{23}, ν_{13}) [Reddy J.N, 1984]. It should be noted that direction 1 indicates the direction parallel to unidirectional fibers while the direction 2 indicates the direction perpendicular to the orientation of fibers and E, G, and ν indicate the Young's modulus, shear modulus, and Poisson's ratio respectively. The strain vector and thermal strain vector are given as $\{\varepsilon\}=\begin{bmatrix}\varepsilon_{xx} & \varepsilon_{yy} & \gamma_{xy} & \gamma_{yz} & \gamma_{zx}\end{bmatrix}^T$ and $\left\{\varepsilon^{Th}\right\}=\begin{bmatrix}\alpha_{xx}T & \alpha_{yy}T & \alpha_{xy}T & 0 & 0\end{bmatrix}^T$ respectively. The effect of temperature field is considered along with the in-plane strain components. The quantities α_{xx}, α_{yy} and α_{xy} are the thermal expansion coefficients in the plate co-ordinates.

3.5. Analytical modelling of composite plates in thermo-mechanical environment

The governing differential equations for the thermo-mechanical analysis of laminated composite plates are developed using the principle of virtual work and employing fundamental laws of calculus of variation.

$$\int_0^T (\delta U + \delta W) = 0 \tag{3.6}$$

where δU is the virtual strain energy and δW is the virtual work done due to applied load on the laminated plate. The virtual strain energy expression and virtual work done due to imposed forces are obtained as:

$$\delta U = \int_{\Omega_0} \left\{ \int_{\frac{-h}{2}}^{\frac{h}{2}} \left[\sigma_{xx}\delta\varepsilon_{xx} + \sigma_{yy}\delta\varepsilon_{yy} + \tau_{xy}\delta\gamma_{xy} + \tau_{yz}\delta\gamma_{yz} + \tau_{xz}\delta\gamma_{xz} \right] dz \right\} dxdy \tag{3.7}$$

$$\delta W = \int_{\Omega_0} q\delta w_0 dxdy \tag{3.8}$$

The virtual work statement given in Eq. (36) is solved variationally after substituting Eqs. (3.5, 3.7-8) and using fundamental lemma of variation. It should be noted that all the variations are arbitrary and hence there corresponding co-efficient must vanish. In this process, the set of five differential equations is obtained in terms of stress and moment resultants and is given as:

$$\frac{\partial N_{xx}}{\partial x}+\frac{\partial N_{xy}}{\partial y}=\frac{\partial N_{xx}^{T}}{\partial x}+\frac{\partial N_{xy}^{T}}{\partial y}$$

$$\frac{\partial N_{yy}}{\partial y}+\frac{\partial N_{xy}}{\partial x}=\frac{\partial N_{yy}^{T}}{\partial y}+\frac{\partial N_{xy}^{T}}{\partial x}$$

$$\frac{\partial^2 M_{xx}}{\partial x^2}+\frac{\partial^2 M_{yy}}{\partial y^2}+2\frac{\partial^2 M_{xy}}{\partial x\partial y}+q=\frac{\partial^2 M_{xx}^{T}}{\partial x^2}+\frac{\partial^2 M_{yy}^{T}}{\partial y^2}+2\frac{\partial^2 M_{xy}^{T}}{\partial x\partial y} \tag{3.9}$$

$$\Omega\frac{\partial M_{xx}}{\partial x}+\frac{\partial P_{xx}}{\partial x}+\Omega\frac{\partial M_{xy}}{\partial y}+\frac{\partial P_{xy}}{\partial y}-\Omega S_1-K_1=\Omega\frac{\partial M_{xx}^{T}}{\partial x}+\frac{\partial P_{xx}^{T}}{\partial x}+\Omega\frac{\partial M_{xy}^{T}}{\partial y}+\frac{\partial P_{xy}^{T}}{\partial y}$$

$$\Omega\frac{\partial M_{yy}}{\partial y}+\frac{\partial P_{yy}}{\partial y}+\Omega\frac{\partial M_{xy}}{\partial x}+\frac{\partial P_{xy}}{\partial x}-\Omega S_2-K_2=\Omega\frac{\partial M_{yy}^{T}}{\partial y}+\frac{\partial P_{yy}^{T}}{\partial y}+\Omega\frac{\partial M_{xy}^{T}}{\partial x}+\frac{\partial P_{xy}^{T}}{\partial x}$$

The stress and couple resultants appearing in Eq. (3.9) are identified as

$$\begin{bmatrix} N_{xx} & M_{xx} & P_{xx} \\ N_{yy} & M_{yy} & P_{yy} \\ N_{xy} & M_{xy} & P_{xy} \end{bmatrix}=\int_{\frac{-h}{2}}^{\frac{h}{2}}\begin{Bmatrix}\sigma_{xx}\\ \sigma_{yy}\\ \tau_{xy}\end{Bmatrix}\begin{bmatrix}1 & z & g(z)\end{bmatrix}dz \tag{3.10}$$

$$\begin{bmatrix} N_{xx}^{T} & M_{xx}^{T} & P_{xx}^{T} \\ N_{yy}^{T} & M_{yy}^{T} & P_{yy}^{T} \\ N_{xy}^{T} & M_{xy}^{T} & P_{xy}^{T} \end{bmatrix}=\int_{\frac{-h}{2}}^{\frac{h}{2}}\left[Q\right]_{5\times5}^{k}\times\begin{Bmatrix}\alpha_{xx}\\ \alpha_{yy}\\ \alpha_{xy}\\ 0\\ 0\end{Bmatrix}\begin{bmatrix}1 & z & g(z)\end{bmatrix}Tdz \tag{3.11}$$

$$\begin{bmatrix} S_2 & K_2 \\ S_1 & K_1 \end{bmatrix}=\int_{\frac{-h}{2}}^{\frac{h}{2}}\begin{Bmatrix}\tau_{yz}\\ \tau_{xz}\end{Bmatrix}\begin{bmatrix}1 & g'(z)\end{bmatrix}dz \tag{3.12}$$

where N , M and P are in plane stress and moment resultants. The parameters S and K are stress resultants in transverse direction. The superscript T indicates the resultants corresponding to thermal effect. The governing equations as given in Eq. (3.9) are further expressed in terms of primary displacements and rotations by involving the following integrals into the formulation.

$$\begin{bmatrix}A_{ij} & B_{ij} & D_{ij} & E_{ij} & F_{ij} & H_{ij}\end{bmatrix}=\int_{\frac{-h}{2}}^{\frac{h}{2}}\left[Q_{ij}^{k}\right]\begin{bmatrix}1 & z & z^2 & g(z) & z.g(z) & (g(z))^2\end{bmatrix}dz \tag{3.13}$$

$$\left[A_i^T \quad B_i^T \quad D_i^T \quad B_i^{AT} \quad D_i^{AT} \quad F_i^{AT}\right] = \int_{\frac{-h}{2}}^{\frac{h}{2}} \left[Q\right]_{5\times5}^{k} \begin{Bmatrix} \alpha_{xx} \\ \alpha_{yy} \\ \alpha_{xy} \\ 0 \\ 0 \end{Bmatrix} \times \begin{Bmatrix} 1 & z & z^2 & f(z) & z.f(z) & (f(z))^2 \end{Bmatrix} dz \tag{3.14}$$

where *i, j* are 1,2,4,5,6 .

$$\left[K_{ij} \quad L_{ij}\right] = \int_{\frac{-h}{2}}^{\frac{h}{2}} \left[Q_{ij}^{k}\right]_{2\times2} \left[g'(z) \quad (g'(z))^2\right] dz \text{ where } i, j \text{ are 4,5.} \tag{3.15}$$

Substituting Eq. (3.10-15) in Eq. (3.9), the governing equation in the form of displacements is yielded and is written as:

$$\left[R\right]\left\{\Delta\right\} = \left\{F\right\} \tag{3.16}$$

where *R* is a square symmetric matrix of stiffness coefficients, Δ is the generalized displacement vector and *F* is force vector. It should be noted that the most general form of Eq. (3.16) is valid for all lamination sequence. However, in the present work, the analytical solutions for cross-ply and angle-ply laminated composites are sought and therefore Eq. (3.16) and its solution are explicitly presented for cross-ply and angle-ply laminated composite plates in the further sections.

3.5.1 Cross-ply plates : Governing equations and solution methodology

The cross-ply laminated plates are characterized with the following stiffness characteristics:

$$\begin{aligned} &A_{16} = A_{26} = B_{16} = B_{26} = D_{16} = D_{26} = 0 \\ &E_{16} = E_{26} = F_{16} = F_{26} = H_{16} = H_{26} = 0 \\ &A_{45} = B_{45} = D_{45} = E_{45} = F_{45} = H_{45} = K_{45} = L_{45} = 0 \end{aligned} \tag{3.17}$$

The thermal stiffness characteristics associated with cross-ply laminated plates are as follows:

$$A_6^T = B_6^T = D_6^T = B_6^{AT} = D_6^{AT} = F_6^{AT} = 0 \tag{3.18}$$

These characteristics are incorporated into Eq. (3.16) and the explicit equations for cross-ply laminates are as:

$$A_{11}\left(\frac{\partial^2 u_0}{\partial x^2}\right)+B_{11}\left(\Omega\frac{\partial^2\theta_x}{\partial x^2}-\frac{\partial^3 w_0}{\partial x^3}\right)+E_{11}\left(\frac{\partial^2\theta_x}{\partial x^2}\right)+A_{12}\left(\frac{\partial^2 v_0}{\partial x\partial y}\right)$$
$$+B_{12}\left(\Omega\frac{\partial^2\theta_y}{\partial x\partial y}-\frac{\partial^3 w_0}{\partial x\partial y^2}\right)+E_{12}\left(\frac{\partial^2\theta_y}{\partial x\partial y}\right)+A_{66}\left(\frac{\partial^2 u_0}{\partial y^2}+\frac{\partial^2 v_0}{\partial x\partial y}\right)+$$
$$B_{66}\left(\Omega\left(\frac{\partial^2\theta_x}{\partial x^2}+\frac{\partial^2\theta_y}{\partial x\partial y}\right)-2\left(\frac{\partial^3 w_0}{\partial x\partial y^2}\right)\right)+E_{66}\left(\frac{\partial^2\theta_x}{\partial x^2}+\frac{\partial^2\theta_y}{\partial x\partial y}\right)=$$
$$A_1^T\left(\frac{\partial T_1}{\partial x}\right)+B_1^T\left(\frac{\partial T_2}{\partial x}\right)+B_1^{AT}\left(\frac{\partial T_3}{\partial x}\right)+\Omega B_1^T\left(\frac{\partial T_3}{\partial x}\right)$$

$$A_{22}\left(\frac{\partial^2 v_0}{\partial x^2}\right)+B_{22}\left(\Omega\frac{\partial^2\theta_y}{\partial y^2}-\frac{\partial^3 w_0}{\partial y^3}\right)+E_{22}\left(\frac{\partial^2\theta_y}{\partial y^2}\right)+A_{12}\left(\frac{\partial^2 u_0}{\partial x\partial y}\right)+B_{12}\left(\Omega\frac{\partial^2\theta_x}{\partial x\partial y}-\frac{\partial^3 w_0}{\partial x^2\partial y}\right)$$
$$+E_{12}\left(\frac{\partial^2\theta_x}{\partial x\partial y}\right)+A_{66}\left(\frac{\partial^2 u_0}{\partial x\partial y}+\frac{\partial^2 v_0}{\partial x^2}\right)+B_{66}\left(\Omega\left(\frac{\partial^2\theta_x}{\partial x\partial y}+\frac{\partial^2\theta_y}{\partial x^2}\right)-2\left(\frac{\partial^3 w_0}{\partial x^2\partial y}\right)\right)$$
$$+E_{66}\left(\frac{\partial^2\theta_x}{\partial x\partial y}+\frac{\partial^2\theta_y}{\partial x^2}\right)=A_2^T\left(\frac{\partial T_1}{\partial y}\right)+B_2^T\left(\frac{\partial T_2}{\partial y}\right)+B_2^{AT}\left(\frac{\partial T_3}{\partial y}\right)+\Omega B_2^T\left(\frac{\partial T_3}{\partial y}\right)$$

$$B_{11}\left(\frac{\partial^3 u_0}{\partial x^3}\right)+D_{11}\left(\Omega\frac{\partial^3\theta_x}{\partial x^3}-\frac{\partial^4 w_0}{\partial x^4}\right)+F_{11}\left(\frac{\partial^3\theta_x}{\partial x^3}\right)+B_{12}\left(\frac{\partial^3 u_0}{\partial x\partial y^2}+\frac{\partial^3 v_0}{\partial x^2\partial y}\right)$$
$$+D_{12}\left(\Omega\left(\frac{\partial^3\theta_y}{\partial x^2\partial y}+\frac{\partial^3\theta_x}{\partial x\partial y^2}\right)-2\frac{\partial^4 w_0}{\partial x^2\partial y^2}\right)+F_{12}\left(\frac{\partial^3\theta_y}{\partial x^2\partial y}+\frac{\partial^3\theta_x}{\partial x\partial y^2}\right)+B_{22}\left(\frac{\partial^3 v_0}{\partial y^3}\right)$$
$$D_{22}\left(\Omega\frac{\partial^3\theta_y}{\partial y^3}-\frac{\partial^4 w_0}{\partial y^4}\right)+F_{22}\left(\frac{\partial^3\theta_y}{\partial y^3}\right)+2B_{66}\left(\frac{\partial^3 u_0}{\partial x\partial y^2}+\frac{\partial^3 v_0}{\partial x^2\partial y}\right)+2D_{66}\left(\Omega\left(\frac{\partial^3\theta_y}{\partial x^2\partial y}+\frac{\partial^3\theta_x}{\partial x\partial y^2}\right)-2\frac{\partial^4 w_0}{\partial x^2\partial y^2}\right)$$
$$+2F_{66}\left(\frac{\partial^3\theta_y}{\partial x^2\partial y}+\frac{\partial^3\theta_x}{\partial x\partial y^2}\right)+q=B_1^T\left(\frac{\partial^2 T_1}{\partial x^2}\right)+D_1^T\left(\frac{\partial^2 T_2}{\partial x^2}\right)+D_1^{AT}\left(\frac{\partial^2 T_3}{\partial^2 x}\right)+\Omega D_1^T\left(\frac{\partial^2 T_3}{\partial^2 x}\right)$$
$$+B_2^T\left(\frac{\partial^2 T_1}{\partial y^2}\right)+D_2^T\left(\frac{\partial^2 T_2}{\partial y^2}\right)+D_2^{AT}\left(\frac{\partial^2 T_3}{\partial y^2}\right)+\Omega D_2^T\left(\frac{\partial^2 T_3}{\partial y^2}\right) \qquad (3.19)$$

$$\left(\Omega B_{11}+E_{11}\right)\left(\frac{\partial^2 u_0}{\partial x^2}\right)+\left(\Omega D_{11}+F_{11}\right)\left(\Omega\frac{\partial^2\theta_x}{\partial x^2}-\frac{\partial^3 w_0}{\partial x^3}\right)+\left(\Omega F_{11}+H_{11}\right)\left(\frac{\partial^2\theta_x}{\partial x^2}\right)+\left(\Omega B_{12}+E_{12}\right)\left(\frac{\partial^2 v_0}{\partial x\partial y}\right)$$
$$+\left(\Omega D_{12}+F_{12}\right)\left(\Omega\frac{\partial^2\theta_y}{\partial x\partial y}-\frac{\partial^3 w_0}{\partial x\partial y^2}\right)+\left(\Omega F_{12}+H_{12}\right)\left(\frac{\partial^2\theta_y}{\partial x\partial y}\right)+\left(\Omega B_{66}+E_{66}\right)\left(\frac{\partial^2 u_0}{\partial y^2}+\frac{\partial^2 v_0}{\partial x\partial y}\right)+$$
$$\left(\Omega D_{66}+F_{66}\right)\left(\Omega\left(\frac{\partial^2\theta_x}{\partial x^2}+\frac{\partial^2\theta_y}{\partial x\partial y}\right)-2\left(\frac{\partial^3 w_0}{\partial x\partial y^2}\right)\right)+\left(\Omega F_{66}+H_{66}\right)\left(\frac{\partial^2\theta_x}{\partial x^2}+\frac{\partial^2\theta_y}{\partial x\partial y}\right)-\left(\Omega^2 A_{55}+2\Omega K_{55}+L_{55}\right)\theta_x=$$
$$\left(\left(\Omega B_1^T+B_1^{AT}\right)\left(\frac{\partial T_1}{\partial x}\right)+\left(\Omega D_1^T+D_1^{AT}\right)\left(\frac{\partial T_2}{\partial x}\right)+\left(\Omega D_1^{AT}+F_1^{AT}\right)\left(\frac{\partial T_3}{\partial x}\right)+\Omega\left(\Omega D_1^T+D_1^{AT}\right)\left(\frac{\partial T_3}{\partial x}\right)\right)$$

$$(\Omega B_{22}+E_{22})\left(\frac{\partial^2 v_0}{\partial x^2}\right)+(\Omega D_{22}+F_{22})\left(\Omega\frac{\partial^2\theta_y}{\partial y^2}-\frac{\partial^3 w_0}{\partial y^3}\right)+(\Omega F_{22}+H_{22})\left(\frac{\partial^2\theta_y}{\partial y^2}\right)+(\Omega B_{12}+E_{12})\left(\frac{\partial^2 u_0}{\partial x\partial y}\right)$$
$$+(\Omega D_{12}+F_{12})\left(\Omega\frac{\partial^2\theta_x}{\partial x\partial y}-\frac{\partial^3 w_0}{\partial x^2\partial y}\right)+(\Omega F_{12}+H_{12})\left(\frac{\partial^2\theta_x}{\partial x\partial y}\right)+(\Omega B_{66}+E_{66})\left(\frac{\partial^2 u_0}{\partial x\partial y}+\frac{\partial^2 v_0}{\partial x^2}\right)+$$
$$(\Omega D_{66}+F_{66})\left(\Omega\left(\frac{\partial^2\theta_x}{\partial x\partial y}+\frac{\partial^2\theta_y}{\partial x^2}\right)-2\left(\frac{\partial^3 w_0}{\partial x^2\partial y}\right)\right)+(\Omega F_{66}+H_{66})\left(\frac{\partial^2\theta_x}{\partial x\partial y}+\frac{\partial^2\theta_y}{\partial x^2}\right)-(\Omega^2 A_{44}+2\Omega K_{44}+L_{44})\theta_y=$$
$$(\Omega B_2^T+B_2^{AT})\left(\frac{\partial T_1}{\partial y}\right)+(\Omega D_2^T+D_2^{AT})\left(\frac{\partial T_2}{\partial y}\right)+(\Omega D_2^{AT}+F_2^{AT})\left(\frac{\partial T_3}{\partial y}\right)+\Omega(\Omega D_2^T+D_2^{AT})\left(\frac{\partial T_3}{\partial y}\right)$$

The thermo-mechanical behaviour of laminated composite plates is examined by solving the Eq. (3.19). These differential equations are solved in the exact manner implementing Navier solution. The simply supported (SS1) boundary conditions. for the cross-ply plate are indicated in Eq. (3.20). The Navier solution satisfying these boundary conditions is given in Eq. (3.21).

$$u_0 = w_0 = \Theta_x = N_{yy} = M_{yy} = 0 \text{ at } y = 0, b$$
$$v_0 = w_0 = \Theta_y = N_{xx} = M_{xx} = 0 \text{ at } x = 0, a \tag{3.20}$$

$$u_0=\sum_{m=1}^{\infty}\sum_{n=1}^{\infty}U_{mn}\cos(\alpha x)\sin(\beta y)$$
$$v_0=\sum_{m=1}^{\infty}\sum_{n=1}^{\infty}V_{mn}\sin(\alpha x)\cos(\beta y)$$
$$w_0=\sum_{m=1}^{\infty}\sum_{n=1}^{\infty}W_{mn}\sin(\alpha x)\sin(\beta y)$$
$$\theta_x=\sum_{m=1}^{\infty}\sum_{n=1}^{\infty}X_{mn}\cos(\alpha x)\sin(\beta y) \tag{3.21}$$
$$\theta_y=\sum_{m=1}^{\infty}\sum_{n=1}^{\infty}Y_{mn}\sin(\alpha x)\cos(\beta y)$$
$$\alpha=\frac{m\pi}{a},\beta=\frac{n\pi}{b}$$

where U_{mn} ,V_{mn} ,W_{mn} ,$X_{mn,}$ and Y_{mn} are simplified arbitrarily parameters to be determined by substituting the mid plane displacements and rotations in Eq. (3.19). The transverse load and the temperature field applied onto the plate are assumed as

$$
\begin{aligned}
q &= \sum_{m=1}^{\infty}\sum_{n=1}^{\infty} q_{mn} \sin(\alpha x)\sin(\beta y) \\
T_1 &= \overline{T_1} \sin(\alpha x)\sin(\beta y) \\
T_2 &= \overline{T_2} \sin(\alpha x)\sin(\beta y) \\
T_3 &= \overline{T_3} \sin(\alpha x)\sin(\beta y)
\end{aligned}
\tag{3.22}
$$

where $q_{mn} = q_0$ for sinusoidal load and $q_{mn} = (16\, q_0/\pi^2\, mn)$ for uniformly distributed load. The substitution of the assumed solution and assumed loading conditions into differential equations defined in Eq. (3.19) yields the set of simultaneous equations which are solved to obtain the arbitrary parameters. The solution of the parameters (U_{mn} ,V_{mn} ,W_{mn} ,$X_{mn,}$ and Y_{mn}) are obtained in the form

$$
\left\{ \mathrm{U_{mn}} \quad \mathrm{V_{mn}} \quad \mathrm{W_{mn}} \quad \mathrm{X_{mn}} \quad \mathrm{Y_{mn}} \right\}^T = \overline{\left[R^C \right]}^{-1} \left\{ \overline{F^C} \right\} \tag{3.23}
$$

The elements of resultant stiffness matrix $\left[\overline{R^C}\right]$ and force vector $\left\{\overline{F^C}\right\}$ are obtained by implementing the solution. The values obtained from Eq. (3.23) are substituted in Eq. (3.21) to obtain mid plane displacements and rotations which are substituted in strain displacement relationship defined in Eq. (3.3) to obtain the strains. The stresses developed at any point in plate due to loading can be obtained from Eq. (3.5) by substituting the value of strains.

3.5.2. Angle-ply plates: Governing equations and solution methodology

For anti-symmetric angle-ply laminated plates the stiffness characteristics are depicted as follows:

$$
\begin{aligned}
&\mathrm{A_{16}}=\mathrm{A_{26}}=\mathrm{D_{16}}=\mathrm{D_{26}}=0 \\
&\mathrm{B_{11}}=\mathrm{B_{22}}=\mathrm{B_{12}}=\mathrm{B_{66}}=0 \\
&\mathrm{E_{11}}=\mathrm{E_{22}}=\mathrm{E_{12}}=\mathrm{E_{66}}=0 \\
&\mathrm{F_{16}}=\mathrm{F_{26}}=\mathrm{H_{16}}=\mathrm{H_{26}}=0 \\
&\mathrm{A_{45}}=\mathrm{B_{44}}=\mathrm{B_{55}}=\mathrm{D_{45}}=\mathrm{E_{44}}=\mathrm{E_{55}}=\mathrm{F_{45}}=\mathrm{H_{45}}=\mathrm{K_{45}}=\mathrm{L_{45}}=0
\end{aligned}
\tag{3.24}
$$

The thermal stiffness characteristics associated with angle-ply laminated plates are as follows:

$$
A_6^T = B_1^T = B_2^T = D_6^T = B_1^{AT} = B_2^{AT} = D_6^{AT} = F_6^{AT} = 0 \tag{3.25}
$$

The characteristics are incorporated into Eq. (3.16) and represented for angle-ply laminates as

$$A_{11}\left(\frac{\partial^2 u_0}{\partial x^2}\right)+A_{12}\left(\frac{\partial^2 v_0}{\partial x\partial y}\right)+B_{16}\left(\Omega\left(2\frac{\partial^2\theta_x}{\partial x\partial y}+\frac{\partial^2\theta_y}{\partial x^2}\right)-2\left(\frac{\partial^3 w_0}{\partial x\partial y^2}\right)-\frac{\partial^3 w_0}{\partial x^2\partial y}\right)$$
$$+A_{66}\left(\frac{\partial^2 u_0}{\partial y^2}+\frac{\partial^2 v_0}{\partial x\partial y}\right)+E_{16}\left(2\frac{\partial^2\theta_x}{\partial x\partial y}+\frac{\partial^2\theta_y}{\partial x^2}\right)+B_{26}\left(\Omega\frac{\partial^2\theta_y}{\partial y^2}-\frac{\partial^3 w_0}{\partial y^3}\right)+E_{26}\left(\frac{\partial^2\theta_y}{\partial y^2}\right)=$$
$$A_1^T\left(\frac{\partial T_1}{\partial x}\right)+B_6^T\left(\frac{\partial T_2}{\partial y}\right)+B_6^{AT}\left(\frac{\partial T_3}{\partial y}\right)+\Omega B_6^T\left(\frac{\partial T_3}{\partial y}\right)$$

$$A_{12}\left(\frac{\partial^2 u_0}{\partial x\partial y}\right)+A_{22}\left(\frac{\partial^2 v_0}{\partial y^2}\right)+B_{26}\left(\Omega\left(2\frac{\partial^2\theta_x}{\partial y^2}+2\frac{\partial^2\theta_y}{\partial x\partial y}\right)-3\left(\frac{\partial^3 w_0}{\partial x\partial y^2}\right)\right)+$$
$$A_{66}\left(\frac{\partial^2 u_0}{\partial x\partial y}+\frac{\partial^2 v_0}{\partial x^2}\right)+E_{26}\left(\frac{\partial^2\theta_x}{\partial y^2}+2\frac{\partial^2\theta_y}{\partial x\partial y}\right)+B_{16}\left(\Omega\frac{\partial^2\theta_y}{\partial x^2}-\frac{\partial^3 w_0}{\partial x^3}\right)+E_{16}\left(\frac{\partial^2\theta_y}{\partial x^2}\right)=$$
$$A_2^T\left(\frac{\partial T_1}{\partial y}\right)+B_6^T\left(\frac{\partial T_2}{\partial x}\right)+B_6^{AT}\left(\frac{\partial T_3}{\partial x}\right)+\Omega B_6^T\left(\frac{\partial T_3}{\partial x}\right)$$

$$B_{16}\left(2\frac{\partial^3 u_0}{\partial x^2\partial y}+\frac{\partial^3 v_0}{\partial x^3}\right)+D_{11}\left(\Omega\frac{\partial^3\theta_x}{\partial x^3}-\frac{\partial^4 w_0}{\partial x^4}\right)+F_{11}\left(\frac{\partial^3\theta_x}{\partial x^3}\right)+$$
$$+D_{12}\left(\Omega\left(\frac{\partial^3\theta_y}{\partial x^2\partial y}+\frac{\partial^3\theta_x}{\partial x\partial y^2}\right)-2\frac{\partial^4 w_0}{\partial x^2\partial y^2}\right)+F_{12}\left(\frac{\partial^3\theta_y}{\partial x^2\partial y}+\frac{\partial^3\theta_x}{\partial x\partial y^2}\right)+B_{22}\left(\frac{\partial^3 v_0}{\partial y^3}\right)$$
$$D_{22}\left(\Omega\frac{\partial^3\theta_y}{\partial y^3}-\frac{\partial^4 w_0}{\partial y^4}\right)+F_{22}\left(\frac{\partial^3\theta_y}{\partial y^3}\right)+B_{26}\left(\frac{\partial^3 u_0}{\partial y^3}+2\frac{\partial^3 v_0}{\partial x\partial y^2}\right)+2D_{66}\left(\Omega\left(\frac{\partial^3\theta_y}{\partial x^2\partial y}+\frac{\partial^3\theta_x}{\partial x\partial y^2}\right)-2\frac{\partial^4 w_0}{\partial x^2\partial y^2}\right)$$
$$+2F_{66}\left(\frac{\partial^3\theta_y}{\partial x^2\partial y}+\frac{\partial^3\theta_x}{\partial x\partial y^2}\right)+q=2B_6^T\left(\frac{\partial^2 T_1}{\partial x\partial y}\right)+D_1^T\left(\frac{\partial^2 T_2}{\partial x^2}\right)+D_1^{AT}\left(\frac{\partial^2 T_3}{\partial^2 x}\right)+\Omega D_1^T\left(\frac{\partial^2 T_3}{\partial^2 x}\right)+D_2^T\left(\frac{\partial^2 T_2}{\partial y^2}\right)$$
$$+D_2^{AT}\left(\frac{\partial^2 T_3}{\partial y^2}\right)+\Omega D_2^T\left(\frac{\partial^2 T_3}{\partial y^2}\right)$$
$$\left(\Omega B_{16}+E_{16}\right)\left(2\frac{\partial^2 u_0}{\partial x\partial y}+\frac{\partial^2 v_0}{\partial x^2}\right)+\left(\Omega D_{11}+F_{11}\right)\left(\Omega\frac{\partial^2\theta_x}{\partial x^2}-\frac{\partial^3 w_0}{\partial x^3}\right)+\left(\Omega F_{11}+H_{11}\right)\left(\frac{\partial^2\theta_x}{\partial x^2}\right)+\left(\Omega B_{26}+E_{26}\right)\left(\frac{\partial^2 v_0}{\partial y^2}\right)$$
$$+\left(\Omega D_{12}+F_{12}\right)\left(\Omega\frac{\partial^2\theta_y}{\partial x\partial y}-\frac{\partial^3 w_0}{\partial x\partial y^2}\right)+\left(\Omega F_{12}+H_{12}\right)\left(\frac{\partial^2\theta_y}{\partial x\partial y}\right)+\left(\Omega D_{66}+F_{66}\right)\left(\Omega\left(\frac{\partial^2\theta_x}{\partial x^2}+\frac{\partial^2\theta_y}{\partial x\partial y}\right)-2\left(\frac{\partial^3 w_0}{\partial x\partial y^2}\right)\right)+$$
$$\left(\Omega F_{66}+H_{66}\right)\left(\frac{\partial^2\theta_x}{\partial x^2}+\frac{\partial^2\theta_y}{\partial x\partial y}\right)-\left(\Omega^2 A_{55}+2\Omega K_{55}+L_{55}\right)\theta_x=$$
$$\left(\left(\Omega B_6^T+B_6^{AT}\right)\left(\frac{\partial T_1}{\partial x}\right)+\left(\Omega D_1^T+D_1^{AT}\right)\left(\frac{\partial T_2}{\partial x}\right)+\left(\Omega D_1^{AT}+F_1^{AT}\right)\left(\frac{\partial T_3}{\partial x}\right)+\Omega\left(\Omega D_1^T+D_1^{AT}\right)\left(\frac{\partial T_3}{\partial x}\right)\right)$$

$$
\begin{aligned}
&(\Omega B_{26}+E_{26})\left(\frac{\partial^2 u_0}{\partial x^2}+2\frac{\partial^2 v_0}{\partial x\partial y}\right)+(\Omega D_{22}+F_{22})\left(\Omega\frac{\partial^2\theta_y}{\partial y^2}-\frac{\partial^3 w_0}{\partial y^3}\right)+(\Omega F_{22}+H_{22})\left(\frac{\partial^2\theta_y}{\partial y^2}\right)+(\Omega B_{16}+E_{16})\left(\frac{\partial^2 u_0}{\partial x^2}\right)\\
&+(\Omega D_{12}+F_{12})\left(\Omega\frac{\partial^2\theta_x}{\partial x\partial y}-\frac{\partial^3 w_0}{\partial x^2\partial y}\right)+(\Omega F_{12}+H_{12})\left(\frac{\partial^2\theta_x}{\partial x\partial y}\right)+(\Omega D_{66}+F_{66})\left(\Omega\left(\frac{\partial^2\theta_x}{\partial x\partial y}+\frac{\partial^2\theta_y}{\partial x^2}\right)-2\left(\frac{\partial^3 w_0}{\partial x^2\partial y}\right)\right)\\
&+(\Omega F_{66}+H_{66})\left(\frac{\partial^2\theta_x}{\partial x\partial y}+\frac{\partial^2\theta_y}{\partial x^2}\right)-(\Omega^2 A_{44}+2\Omega K_{44}+L_{44})\theta_y=\\
&(\Omega B_6^T+B_6^{AT})\left(\frac{\partial T_1}{\partial x}\right)+(\Omega D_2^T+D_2^{AT})\left(\frac{\partial T_2}{\partial y}\right)+(\Omega D_2^{AT}+F_2^{AT})\left(\frac{\partial T_3}{\partial y}\right)+\Omega(\Omega D_2^T+D_2^{AT})\left(\frac{\partial T_3}{\partial y}\right)
\end{aligned}
\tag{3.26}
$$

The Navier solution proposed for angle-ply plate (SS2 conditions) is given in Eq. (3.27).

$v_0 = w_0 = \Theta_x = N_{yy} = M_{yy} = 0$ at $y = 0,b$

$u_0 = w_0 = \Theta_y = N_{xx} = M_{xx} = 0$ at $x = 0,a$

$$
\begin{aligned}
u_0 &= \sum_{m=1}^{\infty}\sum_{n=1}^{\infty} U_{mn}\sin(\alpha x)\cos(\beta y)\\
v_0 &= \sum_{m=1}^{\infty}\sum_{n=1}^{\infty} V_{mn}\cos(\alpha x)\sin(\beta y)\\
w_0 &= \sum_{m=1}^{\infty}\sum_{n=1}^{\infty} W_{mn}\sin(\alpha x)\sin(\beta y)\\
\theta_x &= \sum_{m=1}^{\infty}\sum_{n=1}^{\infty} X_{mn}\cos(\alpha x)\sin(\beta y)\\
\theta_y &= \sum_{m=1}^{\infty}\sum_{n=1}^{\infty} Y_{mn}\sin(\alpha x)\cos(\beta y)\\
\alpha &= \frac{m\pi}{a}, \beta = \frac{n\pi}{b}
\end{aligned}
\tag{3.27}
$$

where U_{mn} ,V_{mn} ,W_{mn} ,$X_{mn,}$ and Y_{mn} are simplified arbitrarily parameters to be determined by substituting the mid plane displacements and rotations in Eq. (3.26).

The transverse load and the temperature field applied onto the plate are assumed as :

$$
\begin{aligned}
q &= \sum_{m=1}^{\infty}\sum_{n=1}^{\infty} q_{mn}\sin(\alpha x)\sin(\beta y)\\
T_1 &= -\overline{T_1}\cos(\alpha x)\cos(\beta y)\\
T_2 &= \overline{T_2}\sin(\alpha x)\sin(\beta y)\\
T_3 &= \overline{T_3}\sin(\alpha x)\sin(\beta y)
\end{aligned}
\tag{3.28}
$$

where $q_{mn} = q_0$ for sinusoidal load and $q_{mn} = (16\ q_0/\pi^2 mn)$ for uniformly distributed load. Substituting assumed solution from Eq. (3.27) and assumed loading conditions from Eq. (3.28) into differential equations defined in Eq.(26) and representing in matrix form, solution of the assumed parameters (U_{mn} ,V_{mn} ,W_{mn} ,$X_{mn,}$ and Y_{mn}) are obtained in the following form:

$$\left\{ \mathrm{U}_{\mathrm{mn}} \quad \mathrm{V}_{\mathrm{mn}} \quad \mathrm{W}_{\mathrm{mn}} \quad \mathrm{X}_{\mathrm{mn}} \quad \mathrm{Y}_{\mathrm{mn}} \right\}^T = \left[\overline{R^A}\right]^{-1}_{5\times5} \left\{\overline{F^A}\right\}_{5\times1} \tag{3.29}$$

The elements of resultant stiffness matrix $\left[\overline{R^A}\right]$ and force vector $\left\{\overline{F^A}\right\}$ are obtained in the similar fashion as $\left[\overline{R^C}\right]$ and $\left\{\overline{F^C}\right\}$ by implementing the stiffness characteristics of angle-ply plates. The values obtained from Eq. (3.29) are substituted in Eq. (3.26) to obtain the mid plane displacements and rotations which can be substituted in strain displacement relationship defined in Eq. (3.3) to obtain the strains. The stresses developed at any point in plate due to loading can be obtained from Eq. (3.5) by substituting the corresponding values of strains.

3.6. Modelling of composite plates in thermo-mechanical environment using finite element method

The closed form solution is only applicable to the simply supported boundary conditions and moreover separate formulation had to be done for cross-ply and angle-ply plates. In order to overcome the limitations of analytical method and to study the effect of boundary conditions on thermo-mechanical response of cross-ply and angle-ply composite plates, the multi-layered composite plates are modelled using finite element method

In order to formulate the finite element modal for thermo-mechanical analysis of laminated plates, the displacement field of IHSDT depicted in Eq. (3.1) has a requirement of C^1 continuity as the displacement field has first order derivative of mid plane transverse deflection (w_0). But C^1 continuity requires very high computational facility as the computational cost and time associated with C^1 continuity is very high. In order to reduce the computational expenses, the continuity requirement is reduced to C^0 continuity. The essential requirement for C^0 continuity is to express the derivatives of mid plane transverse deflection into separate primary variables. The continuity requirement is reduced to C^0 continuity by introducing two new degrees of freedom (ϕ_x, ϕ_y) into displacement field and the displacement field defined in Eq.(3.1) is modified to the form:

$$u(x,y,z) = u_0(x,y) - z\phi_x + f(z)\theta_x$$

$$v(x,y,z) = v_0(x,y) - z\phi_y + f(z)\theta_y \tag{3.30}$$

$$w(x,y,z) = w_0(x,y)$$

Due to the introduction of two separate variables (ϕ_x, ϕ_y), artificial constraints arisen are imposed in the to the total potential energy of the system in following manner:

$$\frac{\partial w_0}{\partial x} - \phi_x = 0 \ , \qquad \frac{\partial w_0}{\partial y} - \phi_y = 0 \tag{3.31}$$

3.6.1. Strain displacement relations

The laminated composite plates are considered to be constituted of the composite material which undergoes linear deformation. Therefore, linear strain-displacement relations as indicated in Eq. (3.32) are implemented for depicting the structural kinematics for the modified displacement field.

$$\varepsilon_{xx} = \frac{\partial u}{\partial x} = \frac{\partial u_0}{\partial x} - z\frac{\partial \phi_x}{\partial x} + (g(z) + \Omega z)\frac{\partial \theta_x}{\partial x}$$

$$\varepsilon_{yy} = \frac{\partial v}{\partial y} = \frac{\partial v_0}{\partial y} - z\frac{\partial \phi_y}{\partial y} + (g(z) + \Omega z)\frac{\partial \theta_y}{\partial y}$$

$$\gamma_{xy} = \frac{\partial u}{\partial y} + \frac{\partial v}{\partial x} = \frac{\partial u_0}{\partial y} + \frac{\partial v_0}{\partial x} - z\frac{\partial \phi_x}{\partial y} - z\frac{\partial \phi_y}{\partial x} + (g(z) + \Omega z)\left(\frac{\partial \theta_x}{\partial y} + \frac{\partial \theta_y}{\partial x}\right) \tag{3.32}$$

$$\gamma_{xz} = \frac{\partial u}{\partial z} + \frac{\partial w}{\partial x} = -\phi_x + (g'(z) + \Omega)\theta_x + \frac{\partial w_0}{\partial x}$$

$$\gamma_{yz} = \frac{\partial v}{\partial z} + \frac{\partial w}{\partial y} = \phi_y + (g'(z) + \Omega)\theta_y + \frac{\partial w_0}{\partial y}$$

The parameters ε_{xx} and ε_{yy} are normal strains in *x* and *y* direction respectively, γ_{xy} is the in-plane shear strain while γ_{xz} and γ_{yz} are the transverse shear strains.

The in-plane normal and shear strains are expressed in the terms of generalised strains as follows:

$$\begin{aligned}
\varepsilon_{xx} &= \varepsilon_1^0 + z\kappa_1^0 + g(z)\kappa_1^1 \\
\varepsilon_{yy} &= \varepsilon_2^0 + z\kappa_2^0 + g(z)\kappa_2^1 \\
\varepsilon_{xy} &= \varepsilon_6^0 + z\kappa_6^0 + g(z)\kappa_6^1 \\
\varepsilon_{xz} &= \varepsilon_4^0 + g'(z)\kappa_4^2 + \Omega\kappa_4^2 \\
\varepsilon_{yz} &= \varepsilon_5^0 + g'(z)\kappa_5^2 + \Omega\kappa_5^2
\end{aligned} \tag{3.33}$$

where

$$\varepsilon_1^0 = \frac{\partial u_\circ}{\partial x}, \quad \kappa_1^0 = \Omega\frac{\partial \theta_x}{\partial x} - \frac{\partial \phi_x}{\partial x}, \quad \kappa_1^1 = \frac{\partial \theta_x}{\partial x}$$

$$\varepsilon_2^0 = \frac{\partial v_\circ}{\partial y}, \quad \kappa_2^0 = \Omega\frac{\partial \theta_x}{\partial y} - \frac{\partial \phi_x}{\partial y}, \quad \kappa_2^1 = \frac{\partial \theta_x}{\partial y}$$

$$\varepsilon_6^0 = \frac{\partial v_\circ}{\partial x} + \frac{\partial u_\circ}{\partial y}, \quad \kappa_6^0 = \Omega\left(\frac{\partial \theta_x}{\partial y} + \frac{\partial \theta_y}{\partial x}\right) - \left(\frac{\partial \phi_x}{\partial y} + \frac{\partial \phi_y}{\partial x}\right), \kappa_6^1 = \left(\frac{\partial \theta_x}{\partial y} + \frac{\partial \theta_y}{\partial x}\right)$$

$$\varepsilon_4^0 = \frac{\partial w_\circ}{\partial y} - \phi_y, \kappa_4^2 = \theta_y$$

$$\varepsilon_5^0 = \frac{\partial w_\circ}{\partial x} - \phi_x, \kappa_5^2 = \theta_y$$

The strain vector $\{\varepsilon\}$ can be represented in the form:

$$\{\varepsilon\}_{5\times 1} = [H]_{5\times 13}\{\overline{\varepsilon_i}\}_{13\times 1} \tag{3.34}$$

where

$$\{H\} = \begin{Bmatrix}
1 & 0 & 0 & z & 0 & 0 & g(z) & 0 & 0 & 0 & 0 & 0 & 0 \\
0 & 1 & 0 & 0 & z & 0 & 0 & g(z) & 0 & 0 & 0 & 0 & 0 \\
0 & 0 & 1 & 0 & 0 & z & 0 & 0 & g(z) & 0 & 0 & 0 & 0 \\
0 & 0 & 0 & 0 & 0 & 0 & 0 & 0 & 0 & 1 & 0 & g'(z) & 0 \\
0 & 0 & 0 & 0 & 0 & 0 & 0 & 0 & 0 & 0 & 1 & 0 & g'(z)
\end{Bmatrix}$$

and

$$\{\bar{\varepsilon}_i\} = \{\varepsilon_1^0 \quad \varepsilon_2^0 \quad \varepsilon_6^0 \quad \kappa_1^0 \quad \kappa_2^0 \quad \kappa_6^0 \quad \kappa_1^1 \quad \kappa_2^1 \quad \kappa_6^1 \quad \varepsilon_4^0 \quad \varepsilon_5^0 \quad \kappa_4^2 \quad \kappa_5^2\}$$

3.6.2. Selection of the element

An iso-parametric serendipity biquadratic element having eight nodes is taken for meshing the considered plate geometry. At each node of the element, seven degrees of freedom is considered for ensuring the continuity requirement. The shape functions for i^{th} node of the considered element are as follows:

$$N_i = \begin{cases} \frac{1}{4}(1+\xi\xi_i)(1+\eta\eta_i)(\xi\xi_i+\eta\eta_i-1) & \text{for} \quad i=1,2,3,4 \\ \frac{1}{2}(1-\xi^2)(1+\eta\eta_i) & \text{for} \quad i=5,7 \\ \frac{1}{2}(1-\eta^2)(1+\xi\xi_i) & \text{for} \quad i=6,8 \end{cases} \tag{3.35}$$

Thus, the field variables and element geometry can be expressed in the terms shape functions of each node of the element as:

$$q = \sum_{i=1}^{8} N_i q_i \text{ and } \xi = \sum_{i=1}^{8} N_i \xi_i \tag{3.36}$$

where the parameter q denotes the generalised field variable, q_i denotes the corresponding value of the field variable at i^{th} node of the element. In the same manner, ς denotes the generalised geometrical co-ordinate and ς_i denotes the value of geometrical co-ordinate at i^{th} node of the element.

3.6.3. Derivation of strain energy

In order to derive the strain energy the generalized strain vector $\{\bar{\varepsilon}\}$ defined in Eq. (3.34) is expressed in terms of basic field variables $(u_0, v_0, w_0, \theta_x, \theta_y, \phi_x, \phi_y)$ as follows:

$$\{\bar{\varepsilon}_i\}_{13\times1} = \{L\}_{13\times7}\{q\}_{7\times1} \tag{3.37}$$

where $\{q\}=\{u_0 \;\; v_0 \;\; w_0 \;\; \theta_x \;\; \theta_x \;\; \phi_x \;\; \phi_x\}^T$

By making use of Eq. (3.36) and Eq. (337), strain displacement relationship for lth element as follows:

$$\{\bar{\varepsilon}_i\}_l = \{B\}_l \{q\}_l \tag{3.38}$$

The strain energy due to the strains for the *l*th element can be obtained using the Eqs. (3.34) and (3.38) along with the constitutive relations for the orthotropic plate as follows:

$$U^{(l)} = \frac{1}{2}\int_V \{\varepsilon\}_l^T \{\sigma\} dV = \frac{1}{2}\int_V \{\varepsilon\}_l^T \{\bar{Q}_{il}\}\{\varepsilon\}_l dV = \frac{1}{2}\int_V \{\varepsilon_i\}_l^T \{H\}_l^T \{\bar{Q}_{il}\}\{H\}_l \{\varepsilon_i\}_l dV$$

$$= \frac{1}{2}\int_S \{q\}_l^T \{B\}_l^T \{D\}_l \{B\}_l \{q\}_l dxdy = \frac{1}{2}\int_S \{q\}_l^T \{K\}_l \{q\}_l dxdy \tag{3.39}$$

By performing assembling for total number of elements (*NL*), the total strain energy (U_T) can be obtained as follows:

$$U_T = \sum_{l=1}^{NL} U^{(l)} = \frac{1}{2}\{q\}^T \{K\}\{q\} \tag{3.40}$$

3.6.4. Work done due to thermal and transverse load

The total work done (W^T) due to thermal and transverse load is obtained as:

$$W^T = \sum_{l=1}^{NL} W_l^{(e)} + \sum_{l=1}^{NL} W_l^{(TH)} = \sum_{l=1}^{NL} \{f^{(e)}\}_l \{q\}_l + \sum_{l=1}^{NL} \{B\}_l^T \{D^{th}\}_l \{q\} \tag{3.41}$$

where $W^{(e)}$ and $W^{(TH)}$ are external work done due to transverse and thermal load respectively. $\{f\} = \{0\ \ 0\ \ p_0\ \ 0\ \ 0\ \ 0\ \ 0\}$ and p_0 is the transverse load applied on to the laminated plate and $D^{th} = \int H_l^T \{\bar{Q}_{il}\}\{\varepsilon^{Th}\}_l dz$.

3.7. Summery

The composite laminated plates are modelled in analytical and finite element framework. The linearly and non-linearly varying thermal load is considered and the governing equations are obtained using the principle of virtual work. The governing equations are solved analytically for simply supported case using Navier type closed form solution differently for cross-ply and angle-ply plates. Further, the laminated plates are modelled in the finite elment framework using the potential energy approach for both cross-ply and angle-ply plates.

CHAPTER-4 RESULTS AND DISCUSSION

4.1. Introduction

The mathematical model proposed and the developed solution methodology is implemented in this section to examine the thermo-mechanical response characteristics of laminated composite plates. The closed form solutions for cross-ply and angle-ply laminates are obtained and various numerical examples are considered to validate the present methodology. The effects of lamination sequence, span thickness ratio, aspect ratio, static loading conditions, and temperature field on the thermo-mechanical response are investigated. The validation of the present results is ensured by comparing with the existing results available in literature and few new results are also presented. The material properties (MP) of each layer of the laminated plate are as follows:

Material Properties 1 (MP1)

$E_1 / E_2 = 25, G_{12} / E_2 = 0.5, G_{13} / E_2 = 0.5, G_{23} / E_2 = 0.2, \nu_{12} = 0.25$ [Zenkour, 2004]

Material Properties 2 (MP2)

$E_1 / E_2 = 40, G_{12} / E_2 = 0.6, G_{13} / E_2 = 0.6, G_{23} / E_2 = 0.5, \nu_{12} = 0.25$ [Reddy, 1999]

4.2. Thermal analysis of cross-ply laminated plates using the closed form solution

4.2.1. Symmetric cross-ply plates

In order to examine the thermo-mechanical response characteristics of symmetric cross-ply plates, an orthotropic plate and a three-layered symmetric plate with lamination sequence [$0^0/90^0/0^0$] are considered. The orthotropic plate and each equal-thickness layer of three-layered laminate are constituted of MP1. The considered plates are subjected to pure thermal load. The thermal load is considered to be linearly sinusoidal (T_1=T_3=0, q=0). The thermo-mechanical characteristics of the square plates under such loading conditions are observed in terms of non-dimensional maximum transverse deflection. The non-dimensional deflection parameter $\bar{w} = (10wh)/\left(\alpha_{xx}\bar{T}_2 a^2\right)$ is obtained using the developed formulation and the results are compared with the existing results presented by Reddy and Hsu (1980) and Zenkour (2004) in Table 4.1. The analysis is carried out for various span-thickness ratio ranging from

a/h = 5 to 100 thereby ensuring the applicability for thick and thin plates. It should be noted that Reddy and Hsu (1980) presented the analytical solutions using FSDT while Zenkour (2004) implemented the SPT for thermo-mechanical response characteristics. It is observed that the present results using IHSDT agree well with the FSDT [Reddy and Hsu, 1980], HSDT [Zenkour, 2004], and SPT [Zenkour, 2004]. It should be noted that this agreement matches well for moderately thick and thin plates (a/h > 20). However, for thick plates, the difference in results among FSDT, HSDT, SPT, and IHSDT is observed. It is well known that HSDT predicts the results more accurately than FSDT due to consideration of parabolic shear deformation effects. The comparison of HSDT, SPT and the IHSDT reveals that the results due to IHSDT are more accurate while the computational efforts are identical due to same number of degrees of freedom involved.

Table 4.1: Effect of thickness and lamination on maximum dimensionless deflection of simply supported orthotropic and symmetric cross ply [$0^0/90^0/0^0$] square plate subjected to sinusoidal temperature field (MP1, T_2=100, α_{yy}/α_{xx}=3)

a/h	[0^0]				[$0^0/90^0/0^0$]			
	Present	FSDT [Reddy and Hsu, 1980]	HSDT [Zenkour, 2004]	SPT [Zenkour, 2004]	Present	FSDT [Reddy and Hsu, 1980]	HSDT [Zenkour, 2004]	SPT [Zenkour, 2004]
5	1.0693	1.0721	1.0711	1.0708	1.2517	1.2224	1.2452	1.2472
6.3	1.0586	1.0602	1.0597	10595	1.2125	1.18700	1.2057	1.2077
10	1.0435	1.0440	1.0439	1.0438	1.1507	1.1365	1.1463	1.1475
12.5	1.0394	1.0396	1.0396	1.0396	1.1323	1.1224	1.1292	1.1300
20	1.0345	1.0346	1.0346	1.0346	1.1101	1.0158	1.1087	1.1090
25	1.0333	1.0334	1.0334	1.0334	1.1045	1.1018	1.1036	1.1039
50	1.0317	1.0317	1.0317	1.0317	1.0970	1.0963	1.0967	1.0968
100	1.0313	1.0313	1.0313	1.0313	1.0950	1.0949	1.0950	1.0950

Further, the considered plates are subjected to combined thermal and transverse load. The linear sinusoidal thermal load (T_1=T_3=0) and bilinear sinusoidal transverse load are imposed on laminated composite plates. The thermo-mechanical response characteristics of the square plates under such loading conditions are determined in terms of non-dimensional transverse deflection at the centre of the plate.

The non- dimensional transverse deflection parameter $\bar{w}$ is obtained by using the relations mentioned in Eq. (4.1)

Table 4.2: Effect of thickness and lamination on dimensionless deflection of simply supported orthotropic and symmetric cross ply [$0^0/90^0/0^0$] square plate subjected to sinusoidal temperature field and transverse loading (MP1, T_2=100, q=100, α_{yy}/α_{xx}=3, $\alpha_{xx}=10^{-6}$)

a/h	$[0^0]$				$[0^0/90^0/0^0]$			
	Present	FSDT [Reddy and Hsu, 1980]	HSDT [Zenkour, 2004]	SPT [Zenkour, 2004]	Present	FSDT [Reddy and Hsu, 1980]	HSDT [Zenkour, 2004]	SPT [Zenkour, 2004]
5	2.7102	2.8332	2.7769	2.7654	3.4075	3.0377	3.2948	3.3238
6.25	2.1244	2.1868	2.1631	2.1575	2.6317	2.9983	2.5394	2.5637
10	1.4502	1.4671	1.4634	1.4621	1.6845	1.5384	1.6366	1.6493
12.5	1.2877	1.2973	1.2958	1.2951	1.4443	1.3451	1.4115	1.4202
20	1.1082	1.1150	1.1113	1.1111	1.1726	1.1312	1.1587	1.1624
25	1.0663	1.0683	1.0682	1.0681	1.1080	1.0811	1.0989	11013
50	1.0101	1.0105	1.0105	1.0105	1.0206	1.0138	1.0183	1.0189
100	0.9959	0.9962	0.9961	0.9960	0.9966	0.9973	0.9980	0.9982

$$\overline{w} = w\left(\left(\frac{q_0 a^4}{h^3 \lambda}\right) + \left(\frac{\alpha_{xx}\overline{T}_2 a^2}{10h}\right)\right)^{-1} \tag{4.1}$$

where $\lambda = \left(\frac{\pi^4}{12}\right)\left(4G_{12} + \frac{\left(E_1 + (1+\nu_{12})E_2\right)}{1-\nu_{12}\nu_{21}}\right)$

The obtained results are presented in Table 4.2 along with the results reported in the existing literature given by Reddy and Hsu (1980) and Zenkour (2004). As evident from the table, there is a good agreement of results given by IHSDT with that of HSDT and SPT for moderately thick and thin plates (a/h>20). However, for thick plates, the difference in results among FSDT, HSDT, SPT, and IHSDT is observed. The comparison of HSDT, SPT and the IHSDT reveals that the results due to IHSDT are more accurate while the computational efforts are identical due to involvement of same number of degrees of freedom.

The variation of maximum transverse deflection parameter with respect to change in aspect ratio (a/b) and span-thickness ratio for a three-layered symmetric cross-ply plate [$0^0/90^0/0^0$] is

presented in Table 4.3. The considered plate is subjected to linearly sinusoidal thermal load (T_1=T_3=0, q=0). The non-dimensional deflection parameter $\bar{w} = (10wh)/(\alpha_{xx}\bar{T}_2 a^2)$ is obtained using the developed formulation. The results are compared with the results given by Reddy and Hsu (1980) and Zenkour (2004). It is observed from the results that for thin plates, the results given by IHSDT agree accordingly with the FSDT, HSDT, and SPT. The accuracy of IHSDT results is observed from the data presented in the table.

Table 4.3: Effect of aspect ratio and thickness on the maximum dimensionless deflection for three layered symmetric cross ply [0^0/90^0/0^0] rectangular plate subjected to sinusoidal temperature field (MP1, T_2=100, α_{yy}/α_{xx}=3)

a/*h*	Theory	*a*/*b*=1/3	*a*/*b*=1/2	*a*/*b*=1.5	*a*/*b*=2
5	Present	1.1097	1.1740	1.0156	0.7187
	FSDT [Reddy and Hsu,1980]	1.0998	1.1535	1.0157	0.7355
	HSDT [Zenkour, 2004]	1.1073	1.1689	1.0169	0.7237
	SPT [Zenkour, 2004]	1.1081	1.1704	1.0167	0.7225
10	Present	1.0733	1.1029	1.0005	0.7432
	FSDT [Reddy and Hsu,1980]	1.0701	1.0959	0.9973	0.7508
	HSDT [Zenkour, 2004]	1.0724	1.1008	0.9997	0.7455
	SPT [Zenkour, 2004]	1.0726	1.1014	0.9999	0.7449
20	Present	1.0628	1.0814	0.9896	0.7574
	FSDT [Reddy and Hsu,1980]	1.0619	1.0795	0.9883	0.7601
	HSDT [Zenkour, 2004]	1.0625	1.0808	0.9892	0.7583
	SPT [Zenkour, 2004]	1.0626	1.0810	0.9893	0.7581
50	Present	1.0597	1.0750	0.9853	0.7632
	FSDT [Reddy and Hsu,1980]	1.0596	1.0748	0.9851	0.7638
	HSDT [Zenkour, 2004]	10567	1.0750	0.9853	0.7634
	SPT [Zenkour, 2004]	1.0597	1.0750	0.9853	0.7634
100	Present	1.0593	1.0741	0.9847	0.7642
	FSDT [Reddy and Hsu,1980]	1.0593	1.0741	0.9847	0.7643
	HSDT [Zenkour, 2004]	1.0593	1.0741	0.9847	0.7642
	SPT [Zenkour, 2004]	1.0593	1.0741	0.9847	0.7642

The variation in dimensionless deflection with span-thickness ratio for four layered [0^0/90^0/90^0/0^0] simply supported symmetric cross-ply plate subjected to pure thermal load (q = 0) is depicted in Figs. 4.1-2. The plate consists of equal thickness orthotropic layers constituted of MP1. The effect of linear temperature field (T_1=T_3=0, T_2=100) is demonstrated

in Fig. 4.1 while Fig. 4.2 indicates the influence of non linear temperature field (T_1= 0, T_3=T_2=100). The results are compared with SPT [Zenkour, 2004] results. It is observed that there is a close agreement of results given by IHSDT and SPT for linearly varying temperature field as evident in Fig. 4.1. However, in case of non-linear temperature field

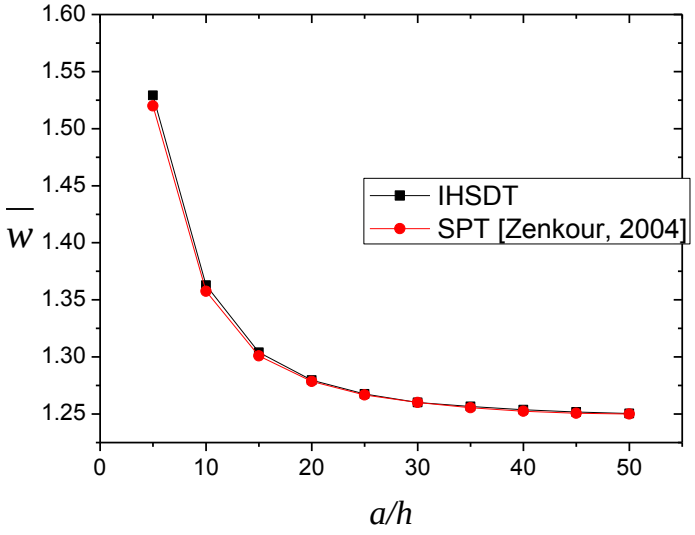

Figure 4.1: Variation of *w* with side to thickness ratio for symmetric cross ply [0^0/90^0/90^0/0^0] plate subjected to sinusoidal temperature field

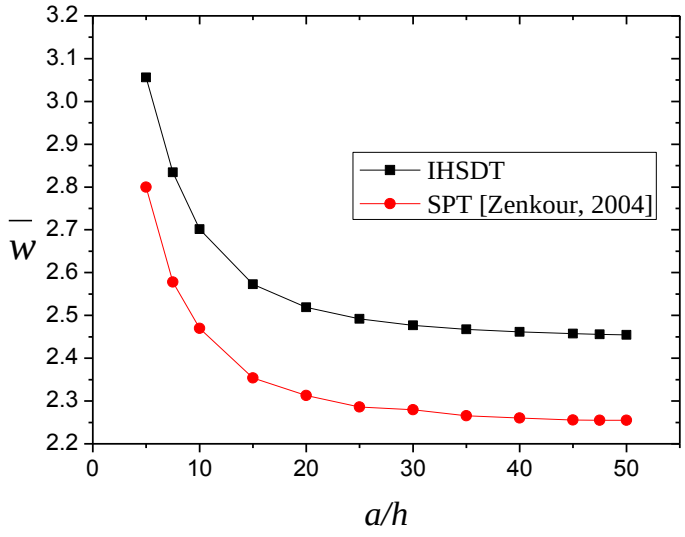

Figure 4.2: Variation in dimensionless deflection at the centre of the plate for symmetric [0^0/90^0/90^0/0^0] cross ply plate (T_3=T_2=100)

there is slight difference in the results given by IHSDT and SPT. This difference in results is due to different non linear functions used in non linear temperature field of SPT and IHSDT.

In order to analyse the effect of non-linear temperature field (T_3) on the dimensionless deflection of the symmetric laminated plate [$0^0/90^0/90^0/0^0$], Fig 4.3 is plotted for thick plate (a/h =10) which shows the variation in dimensionless deflection due to extent of nonlinear temperature field (T_3/T_2). The linear increment in deflection is observed due to increment in the extent of non-linear temperature field (T_3/T_2). It is also observed that the non-dimensional deflection increases by 1.35 times for twice increment in T_3 while T_2 is kept constant. The effect of material anisotropy on dimensionless deflection of four layered [$0^0/90^0/90^0/0^0$] symmetric cross-ply plate (a/h =10) is shown in Fig. 4.4. A linearly varying sinusoidal temperature field is applied on the plate and the results are compared with the results of SPT. IHSDT predicts the deflection with a good agreement with SPT in this case.

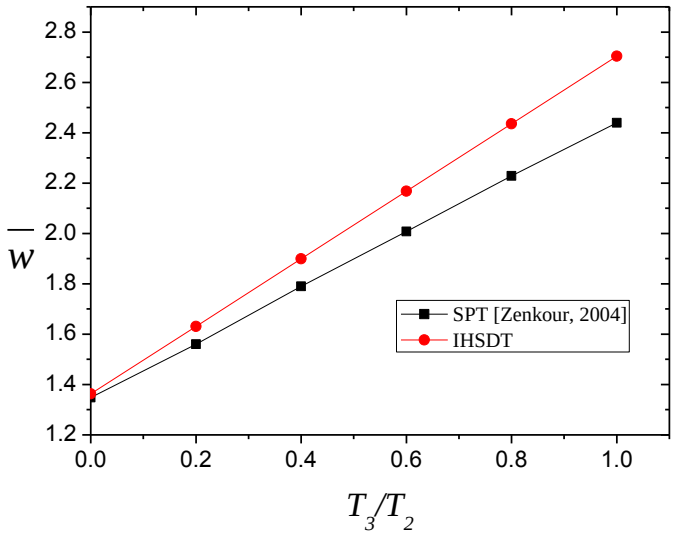

Figure 4.3: Variation in dimensionless deflection with respect to (T_3/T_2) for symmetric cross ply plate [$0^0/90^0/90^0/0^0$]

Fig. 4.5 presents the dimensionless deflection for three layered square symmetric cross-ply plates under various loading conditions. The plate is subjected to transverse loading (q=100, T_1=T_2=T_3=0), pure sinusoidal thermal load (T_2=100, q=T_1 =T_3=0) and combined thermal and mechanical loading (T_1=T_3=0, q = 100, T_2 = 100). The dimensionless deflection in case of pure mechanical loading is lesser in comparison with thermal loading for moderately thicker and thin plates. The deflection due to combined loading is more in comparison with pure mechanical loading for every a/h ratio. For thin plates, the non-dimensional deflection due to

combinedssssss lording is lower than that of non-dimensional deflection due to pure temperature field.

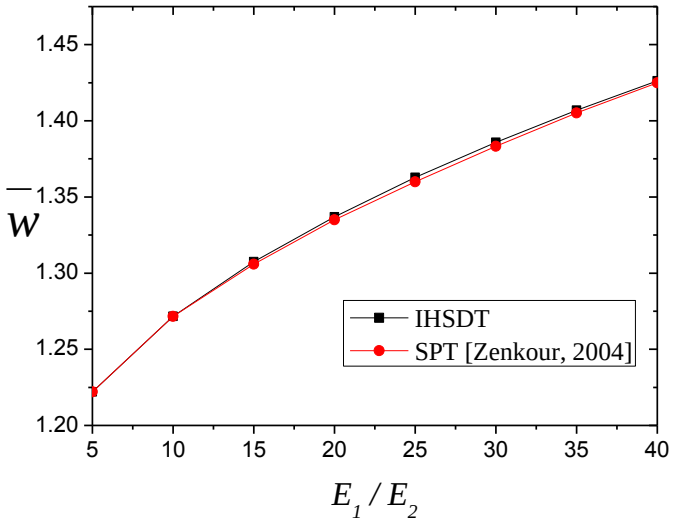

Figure 4.4: Variation of dimensionless deflection with material anisotropy for symmetric cross ply plate $[0^0/90^0/90^0/0^0]$ (T_3=0)

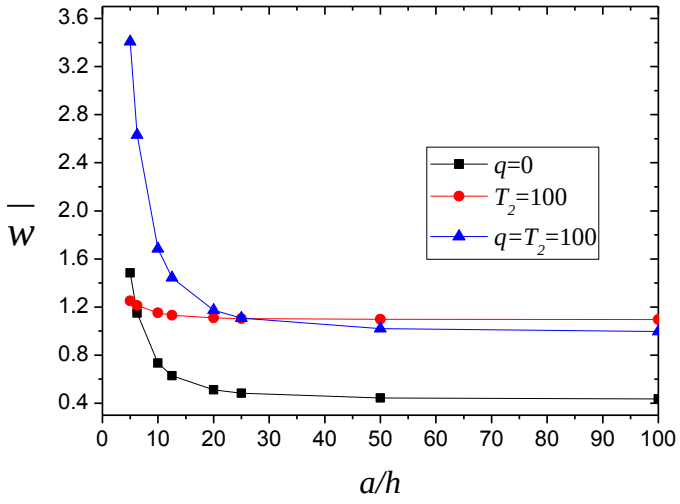

Figure 4.5: Variation of dimensionless deflection with thickness for symmetric cross ply plate $[0^0/90^0/0^0]$ under various loading conditions (T_3=0)

4.2.2. Anti-symmetric cross-ply plates

In order to analyse the thermo-mechanical response characteristics of anti-symmetric cross-ply plates, a two-layered anti-symmetric square plate $[0^0/90^0]$ is considered. The each equal-

thickness layer of two-layered laminate is constituted of MP1. The non-dimensionality relations used are given in Eq. (4.1).

The considered plate is subjected to pure thermal load. The thermal load is linearly sinusoidal (T_1=T_3=0, q=0) in nature. The thermo-mechanical characteristics of the square plates under such loading conditions are examined in terms of maximum transverse deflection. The results are compared with the existing results presented by Reddy and Hsu (1980) and Zenkour(2004) in Table 4.4. It is observed that the present results using IHSDT agree well with the FSDT [Reddy and Hsu, 1980], HSDT [Zenkour, 2004], and SPT [Zenkour, 2004]. It should be noted that the agreement matches well for moderately thick and thin plates (a/h>20). However, for thick plates, the difference in results among FSDT, HSDT, SPT, and IHSDT is observed. It is well known that HSDT predicts the results more accurately than FSDT due to consideration of parabolic shear deformation effects. The comparison of HSDT, SPT and the IHSDT reveals that the results due to IHSDT are more accurate.

Table 4.4: Effect of thickness and lamination on maximum dimensionless deflection of simply supported anti symmetric cross ply [0^0/90^0] square plate subjected to sinusoidal temperature field (MP1, T_2=100, α_{yy}/α_{xx}=3)

a/h	Present	FSDT [Reddy and Hsu, 1980]	HSDT [Zenkour, 2004]	SPT [Zenkour, 2004]
5	1.6955	1.6765	1.6894	1.6910
6.3	1.6888	1.6765	1.6848	1.6858
10	1.6814	1.6765	1.6798	1.6802
12.5	1.6796	1.6765	1.6786	1.6789
20	1.6777	1.6765	1.6773	1.6774
25	1.6773	1.6765	1.6770	1.6771
50	1.6767	1.6765	1.6767	1.6767
100	1.6766	1.6765	1.6766	1.6766

Table 4.5 represents the result for anti-symmetric cross-ply plate under combined thermal and transverse load. The transverse load is sinusoidal load (T_1=T_3=0). The thermo-mechanical characteristics of the square plates under such loading conditions are observed in terms of maximum transverse deflection at the centre of the plate. The results are compared with the

results present in the literature given by Reddy and Hsu (1980) and Zenkour (2004). There is a good agreement of results given by IHSDT with that of HSDT [Zenkour, 2004] and SPT [Zenkour, 2004] for moderately thick and thin plates (a/h>20). The accuracy of IHSDT is clearly observable from the results presented.

Table 4.5: Effect of thickness and lamination on maximum dimensionless deflection of simply supported anti symmetric cross ply [$0^0/90^0$] square plate subjected to sinusoidal temperature field and sinusoidal transverse loading (MP1, T_2=100, q=100, α_{yy}/α_{xx}=3, $\alpha_{xx}=10^{-6}$)

a/h	Present	FSDT [Reddy and Hsu, 1980]	HSDT [Zenkour, 2004]	SPT [Zenkour, 2004]
5	3.6797	4.0415	3.812	3.7821
6.25	3.2433	3.4666	3.3273	3.3090
10	2.7602	2.8438	2.7927	2.7859
12.5	2.6471	27001	2.6679	2.6636
20	2.5240	2.5443	2.5321	2.5304
25	2.4955	2.5083	2.5006	2.4996
50	2.4574	2.4597	2.4586	2.4584
100	2.4478	2.44541	2.4481	2.4481

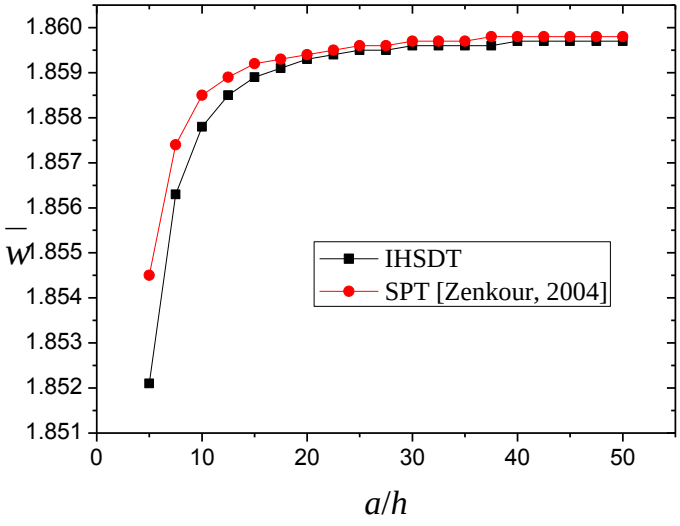

Figure 4.6: Variation of w with side to thickness ratio for anti-symmetric cross ply plate subjected to sinusoidal temperature field

Fig. 4.6 represents the effect of change in side to thickness ratio on dimensionless deflection for four layered [$90^0/0^0/90^0/0^0$] anti-symmetric angle-ply plate subjected to sinusoidal temperature field. The results are compared with SPT [Zenkour, 2004]. It is concluded that for thicker plate again IHSDT under predicts the deflection as compared to SPT, The plate is then subjected to non- linear temperature field (T_3=T_2=100) and the results are presented in Fig. 4.7

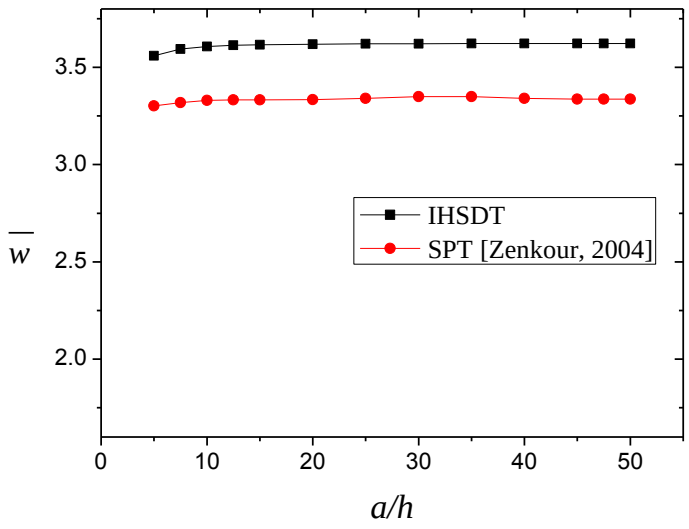

Figure 4.7: Variation in dimensionless deflection at the centre of the plate for anti-symmetric [$90^0/0^0/90^0/0^0$] cross ply plate (T_3=T_2=100)

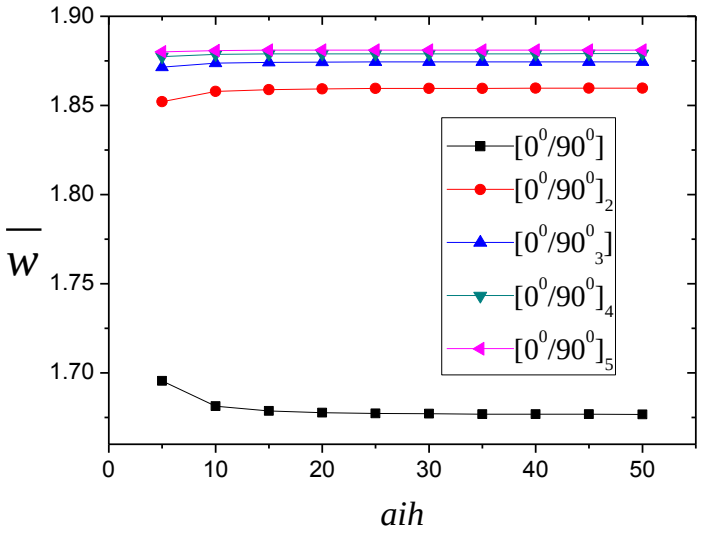

Figure 4.8: Variation in maximum transverse non-dimensional deflection for multilayered anti-symmetric cross ply plate (T_2=100)

Further, the multilayered anti-symmetric cross ply plates are considered and the transverse deflection due to pure thermal load (T_2 = 100) is examined. The analysis is carried out for two, four, six, eight, and ten layered plates aligned in anti-symmetric cross-ply fashion. The results are obtained for varying span-thickness ratio and plotted in Fig. 4.8. It is observed that the dimensionless deflection increases as the number of layers increase. The increase in dimensionless deflection is prominent from two layered plate to four layered plate. However, there is not a significant increase in dimensionless deflection with the increase in number of layers.

4.3. Static analysis of angle-ply laminated composite plates using the closed form solution

In order to examine the static analysis of anti-symmetric angle-ply plates, the simply supported (SS2) anti symmetric angle-ply composite plates having two and six layers with different angles of alignment of fibre orientation are considered. The fiber orientation is taken as 5^0, 30^0, and 45^0. The material properties are taken as specified in MP2.

The plates are subjected to a sinusoidal transverse load. The static response of the square plates under a sinusoidal transverse load is observed in terms of maximum transverse deflection. The non-dimensional deflection parameter $\overline{w} = 100wh^3E_2/qa^4$ is obtained using the developed formulation and the results are compared with the existing results given by third order shear deformation theory (TSDT) [Reddy, 1999] and FSDT [Reddy, 1999] in Table 4.6. It is noticed that for thin plates (a/h>50) the results are well agreed especially for six layer anti-symmetric angle-ply plate. However, there is a notable difference between the results for thicker plates (a/h<20). Since TSDT and IHSDT takes into account the transverse shear effects hence the results due to TSDT and IHSDT are comparatively more accurate than FSDT. It is clear from the results that the IHSDT accurately predicts the results for thicker plates as compared TSDT and FSDT.

The effect of material anisotropy ratio (E_1/E_2) on non-dimensional deflection for [45^0/-45^0] and [45^0/-45^0]$_3$ plates (a/h =10) is presented in Fig. 4.9. The results are compared with TSDT [Reddy, 1999]. It is observed that the results have a good agreement with TSDT. The effect of angle of fibre orientation on the dimensionless deflection of two layered [Θ/-Θ] and six layered [Θ/-Θ]$_3$ square anti-symmetric angle-ply plate is depicted in Fig. 4.10. The fiber

Table 4.6: Effect of fibre orientation and a/h ratio on non dimensional deflection on two and six layer square anti-symmetric angle ply plates subjected to sinusoidal transverse load (MP2)

a/*h*	Theory	5^0		30^0		45^0	
		n=2	*n*=6	*n*=2	*n*=6	*n*=2	*n*=6
	Present	1.1955	1.1689	0.9968	0.8430	0.9326	0.7948
4	TSDT [Reddy, 1999]	1.2625	1.2282	1.0838	0.8851	1.0203	0.8375
	FSDT [Reddy, 1999]	1.3675	1.2647	1.2155	0.8994	1.1576	0.8531
	Present	0.4783	0.4434	0.5794	0.2978	0.5457	0.2718
10	TSDT [Reddy, 1999]	0.4848	0.4485	0.5916	0.3007	0.5587	0.2745
	FSDT [Reddy, 1999]	0.4883	0.4491	0.6099	0.2989	0.5773	0.2728
	Present	0.3565	0.3198	0.5150	0.2121	0.4846	0.1899
20	TSDT [Reddy, 1999]	0.3579	0.3209	0.5180	0.2127	0.4897	0.1905
	FSDT [Reddy, 1999]	0.3586	0.3208	0.5221	0.2121	0.4914	0.1899
	Present	0.3212	0.2840	0.4967	0.1877	0.4699	0.1667
50	TSDT [Reddy, 1999]	0.3215	0.2842	0.4972	0.1878	0.4704	0.1608
	FSDT [Reddy, 1999]	0.3216	0.2840	0.4979	0.1877	0.4712	0.1667
	Present	0.3162	0.2788	0.4941	0.1842	0.4675	0.1638
100	TSDT [Reddy, 1999]	0.3162	0.2789	0.4912	0.1842	0.4676	0.1634
	FSDT [Reddy, 1999]	0.3162	0.2789	0.4914	0.1842	0.4678	0.1638

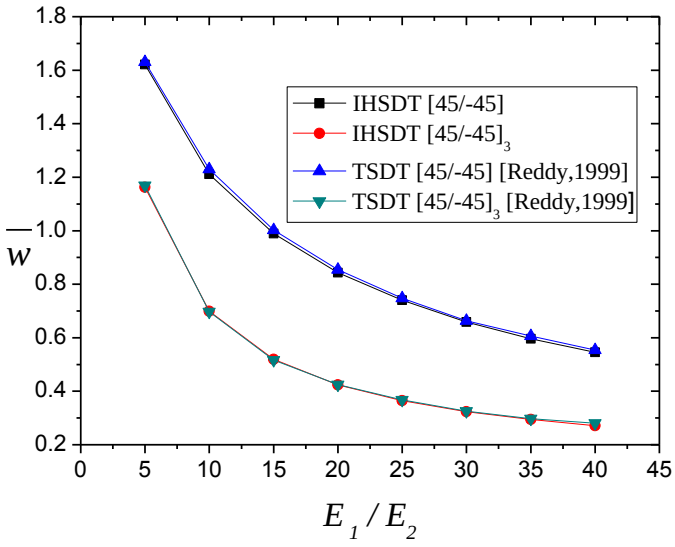

Figure 4.9: Effect of anisotropy on two layer and six layer anti symmetric angle ply square plate

angle is varied from 0^0 to 45^0. The results are compared with FSDT [Reddy, 1999] for *a/h*=10. It is observed that the two layered plate possess higher non-dimensional transverse deflection relative to six layered plate for a particular fiber angle. The non-dimensional deflection decreases for the six layered plate with increase in fiber angle from 0^0 to 45^0. However, it increases till fiber angle of approximately 25^0 and decreases beyond that for two layered plate as indicated in Fig. 4.10.

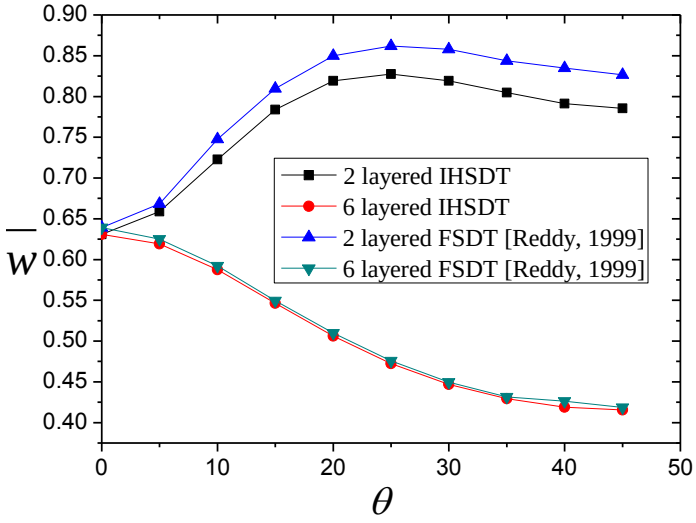

Figure 4.10: Effect of orientation of fibres on two layer and six layer anti symmetric angle ply square

Table 4.7: Effect of fibre orientation and a/h ratio on non dimensional deflection on two layer anti-symmetric rectangular angle ply plates subjected to sinusoidal transverse load (MP2,*b*=3*a*)

a/h	Theory	15^0	30^0	45^0
10	Present	0.9818	1.465	2.2212
	HSDT [Swaminathan and Paul, 2007]	1.0017	1.4872	2.2440
100	Present	0.8016	1.3152	2.0668
	HSDT [Swaminathan and Paul, 2007]	0.8018	1.3154	20673

Further, a two layered rectangular (*b=3a*) anti-symmetric angle-ply plate with fibre orientation of 5^0, 30^0, and 45^0 is considered. The plate is subjected to sinusoidal transverse load. The non-dimensional transverse deflection is obtained and the results are compared with HSDT [Swaminathan and Paul, 2007] in Table 4.7. It is observed that the results are in a good agreement with HSDT for thin plates. However, IHSDT is capable to predict the results

for thick plates more accurately. Also, a two layered [45^0/-45^0] rectangular plate (b = 3a) is considered to determine the stress behaviour. The results for in-plane stresses are presented in Table 4.8 alongwith the results presented by Swaminathan and Ragounadin (2004).

Table 4.8: Effect of a/h ratio on non dimensional stresses on two layer [45^0/-45^0] anti-symmetric rectangular angle ply plates subjected to sinusoidal transverse load (MP2, b=3a)

a/h	Theory	$\bar{\sigma}_{xx}$	$\bar{\sigma}_{yy}$	$\bar{\tau}_{xy}$
4	Present	0.8094	0.6891	-0.4045
	Swaminathan and Ragounadin (2004)	0.9998	0.8794	-0.2816
10	Present	0.7101	0.6004	-0.3764
	Swaminathan and Ragounadin (2004)	0.7437	0.6476	-0.3563
100	Present	0.6901	0.5828	-0.3718
	Swaminathan and Ragounadin (2004)	0.6904	0.5998	-0.3765

The non-dimensional maximum in-plane normal stresses ($\bar{\sigma}_{xx}$ and $\bar{\sigma}_{yy}$) and in are evaluated using the following non-dimensional forms:

$$\bar{\sigma}_{xx}\left(\frac{a}{2},\frac{b}{2},\frac{h}{2}\right)=\sigma_{xx}\left(\frac{h^2}{q_0a^2}\right)$$

$$\bar{\sigma}_{yy}\left(\frac{a}{2},\frac{b}{2},\frac{h}{2}\right)=\sigma_{yy}\left(\frac{h^2}{q_0a^2}\right)$$

4.4. Thermal analysis of anti-symmetric angle ply laminated plates using the closed form solution

In this section, thermal analysis of simply supported anti-symmetric angle ply laminated composite plates is discussed. The two layered, four layered and six layered anti-symmetric angle ply laminated plates with variable angle of fibre orientation are considered. The plates possess the equal thickness orthotropic layered constituted of material properties MP2.

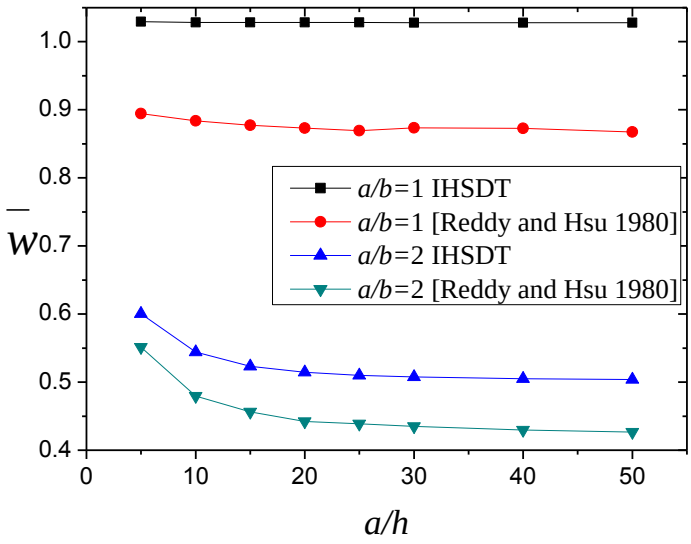

Figure 4.11: Variation in dimensionless deflection of four layered square and rectangular anti-symmetric $[45/-45]_2$ angle ply plate with respect to side to thickness ratio (MP2;T_3=0; $\alpha_{yy}/\alpha_{xx=3}$)

The effect of span-thickness ratio on non-dimensional deflection is examined for four layered anti-symmetric angle ply $[45^0/-45^0/45^0/-45^0]$ plate. The square and rectangular plates (a/b = 2) are subjected to pure thermal load (T_1=T_3=0, q=0, T_2 = 100). The ratio of thermal expansion coefficients (α_{yy}/α_{xx}) is taken as 3. The obtained results are indicated in Fig. 4.11 along with the FSDT results presented by Reddy and Hsu (1980). The significant difference in the present and FSDT results is due to consideration of shear deformation effects in terms of inverse hyperbolic function in the present work. It is observed that the deflection decreases with increase in span-thickness ratio for both configuration. Also, the square plate possesses large non-dimensional deformations relative to considered rectangular plate.

The effect of material anisotropy on the dimensionless deflection of four layered $[45^0/-45^0]_2$ and six layered $[45^0/-45^0]_3$ anti-symmetric angle-ply laminated plates (a/h =10) subjected to sinusoidal temperature field is examined and depicted in Fig. 4.12. It is observed from the results that the dimensionless deflection for six layered plate is lesser in comparison with dimensionless deflection of four layered plate. Moreover there is continues decrease in dimensionless deflection for both the plates with increase in E_1/E_2 ratio. The influence of fiber orientation on non-dimensional deflection of thermally loaded and thermo-mechanically loaded plates anti-symmetric angle ply plates (a/h =10) is shown in Fig 4.13.

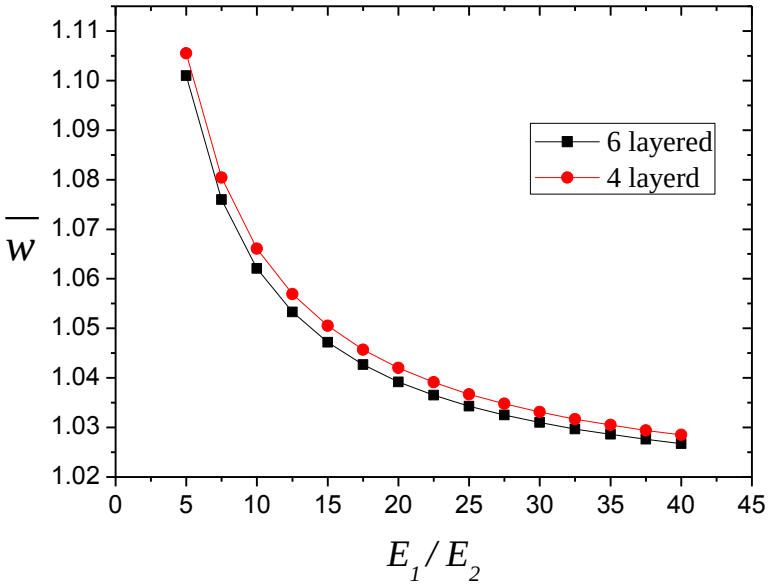

Figure 4.12: Variation in dimensionless deflection of four layered $[45/-45]_2$ and six layered $[45/-45]_3$ square anti-symmetric angle ply plate with change in material anisotropy (MP2;T_3=0; α_{yy}/α_{xx}=3)

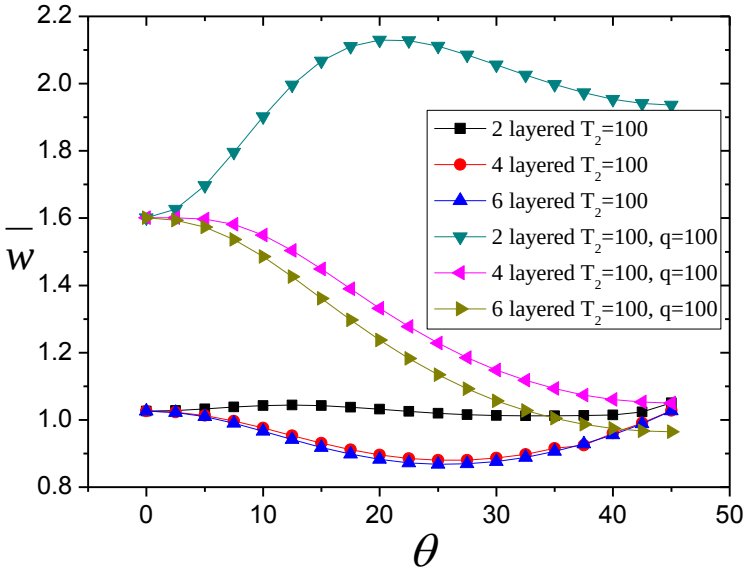

Figure 4.13: Variation in dimensionless deflection of two [θ /- θ], four$[\theta /- \theta]_2$ and six layered $[\theta /- \theta]_3$ square anti-symmetric angle ply plate with change in angle of fibre orientation under various loading conditions(MP2;T_3=0; α_{yy}/α_{xx}=3)

Also, the effect of increase in number of layers is observed. The plates are first subjected to pure thermal load (T_1=T_3=0, q=0, T_2=100) and then to combined thermal and mechanical loading (T_1=T_3=0, q=100, T_2=100). It is concluded that there is an increase in deflection when

the plates are subjected to combined loading as compared to plates subjected to pure thermal load. The dimensionless deflection decreases with the increment in number of layers for a particular fiber orientation and loading condition.

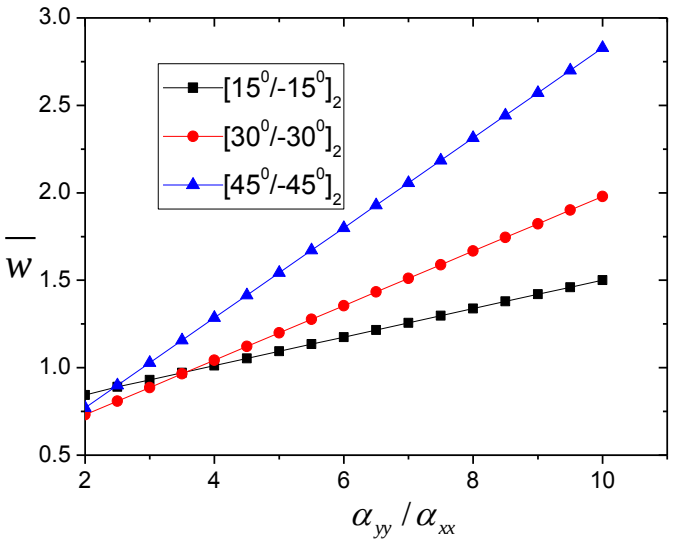

Figure 4.14: Variation in dimensionless deflection of four layered $[\theta/-\theta]_2$ square anti-symmetric angle ply plate with change in α_{yy}/α_{xx} (MP2;T_3=0;)

The effect of increment in the ratio of thermal expansion coefficient (α_{yy}/α_{xx}) on the non-dimensional deflection is observed for the four layered $[\theta/-\theta]_2$ square anti-symmetric angle-ply plates (a/h =10) subjected to sinusoidal temperature field. The fiber orientation is taken as 15^0, 30^0 and 45^0. The obtained results are plotted in Fig. 4.14. It is observed that the dimensionless deflection increases linearly with increase in α_{yy}/α_{xx} ratio. However, the rate of increment is higher for high fiber orientation.

The effect of change in loading condition for a four layered square $[45^0/-45^0]_2$ anti-symmetric angle ply plate is indicated in Fig. 4.15 for a range of span thickness ratio (a/h = 5 to 50). The plate is subjected first to pure mechanical loading (q=100, T_1=T_2=T_3=0) and combined thermal and mechanical loading (T_1=T_3=0, q=100, T_2= 100). It is observed that the plate subjected to combined mechanical and thermal load undergoes large deformation relative to the plate subjected to pure mechanical load. Also, the application of thermal load influences the non-dimensional deflection of thick plates relatively more as compared to thin plates.

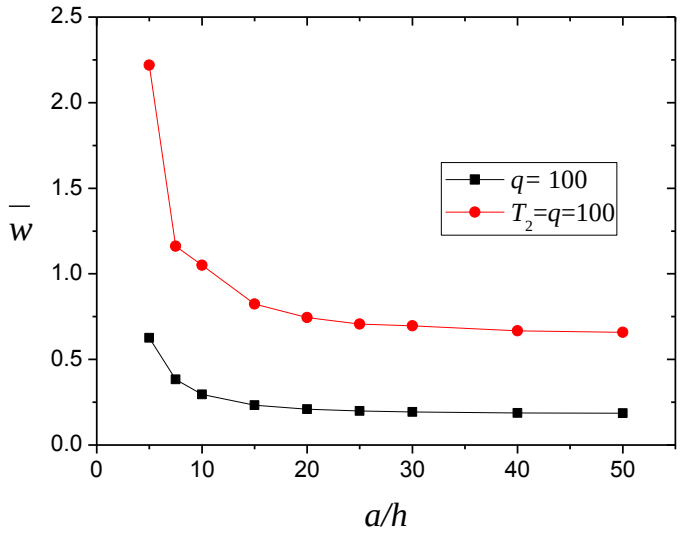

Figure 4.15: Effect of loading conditions on dimensionless deflection of four layered $[45^0/-45^0]_2$ square anti-symmetric angle ply plate

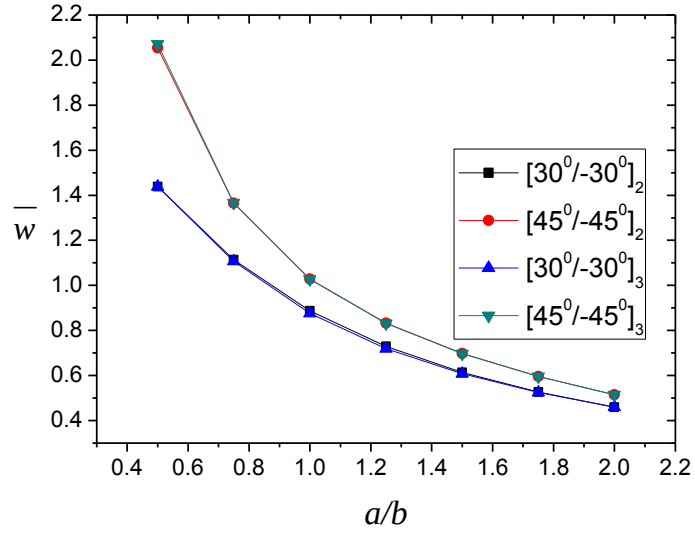

Figure 4.16: Variation in dimensionless deflection of four layered $[30/-30]_2$, $[45/-45]_2$ and six layered $[30/-30]_3$, $[45/-45]_3$ anti-symmetric angle ply plates with aspect ratio

Further, the effect of plate aspect ratio on the non-dimensional transverse deflection of anti-symmetric angle ply plates is considered. The plates are subjected to sinusoidal temperature field varying linearly (T_2 =100) along the thickness. The results are obtained for four layered and six layered anti-symmetric angle-ply plates with fibre orientation of 30^0 and 45^0. Fig. 4.16 depicts the effect of aspect ratio on dimensionless deflection for the considered plate

with a/h =10. It is observed that the non dimensional deflection decreases with increase in aspect ratio.

4.5. Thermo-mechanical analysis of laminated composite plates using finite element method

The present finite element modal for investigating thermo-mechanical response characteristics of cross-ply and angle-ply laminates is validated by comparing with the closed form solution for simply supported boundary conditions. A variety of examples are considered for various boundary conditions for parametric studies. A generalised MATLAB code developed in order to formulate stiffness matrix and force vector for both cross-ply and angle-ply plates. The restrictions of degrees of freedom for various boundary conditions are as follows:

1. Clamped conditions (C): $u_0 = v_0 = w_0 = \phi_x = \phi_y = \theta_x = \theta_y = 0$

2. Simply supported conditions (S) :

$u_0 = w_0 = \phi_x = \theta_x = 0$ for edges parallel to x axis (x=0,a)

$v_0 = w_0 = \phi_y = \theta_y = 0$ for edges parallel to y axis (y=0,b)

4.5.1. Thermo-mechanical analysis of anti-symmetric cross-ply plates

In order to investigate the thermo-mechanical response of anti-symmetric cross-ply plates, two layered anti-symmetric [$0^0/90^0$] square plate is considered. The plate is considered under sinusoidal thermal load linearly varying through the thickness (T_1=T_3=0, q=0). Both the layers of the plate are consisted of MP1. The response characteristics are evaluated in terms of non-dimensional deflection parameter $\overline{w}$ defined in Eq. (4.1)

It should be noted that the maximum transverse non-dimensional deflection is evaluated at the nodal point at the centre of the plate. The non-dimensional deflection is evaluated for different boundary conditions (SSSS, SCSS, SCSC) for different mesh sizes in order to

ensure the convergence of present finite element formulation. The convergence behaviour for non-dimensional deflection for the plate having span to thickness ratio (a/h) equal to 100 is

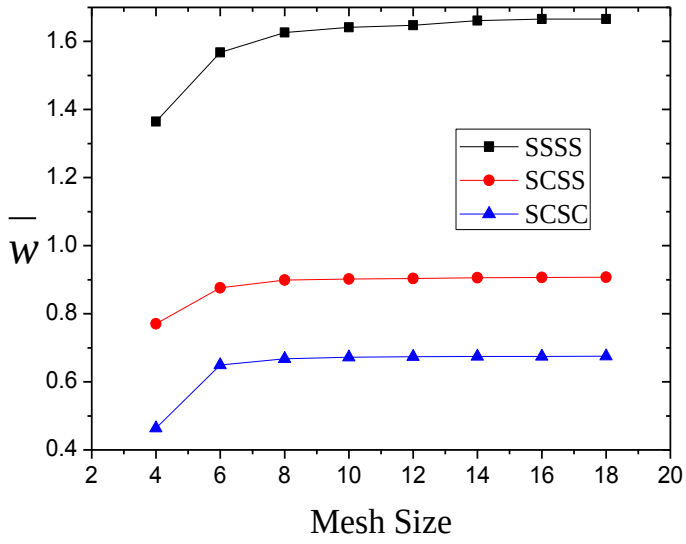

Figure 4.17: Convergence for the non-dimensional deflection of two layered anti-symmetric [$0^0/90^0$] laminated square plate subjected to sinusoidal temperature field (a/h=100, MP1)

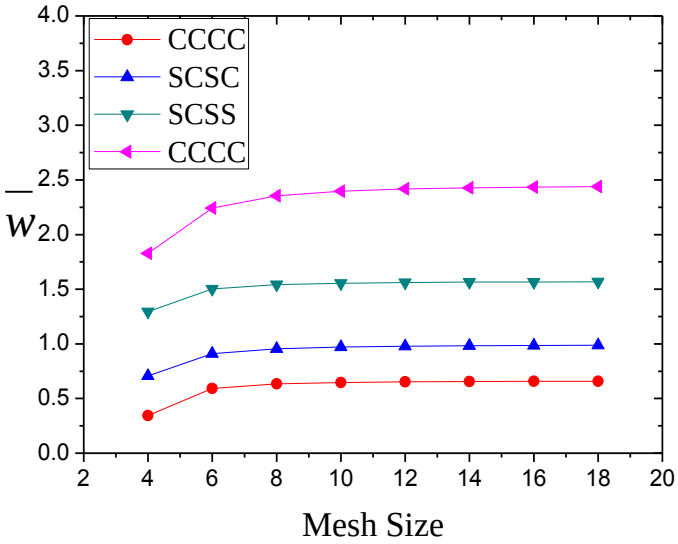

Figure 4.18: Convergence for the non-dimensional deflection of two layered anti-symmetric [$0^0/90^0$] laminated square plate subjected to sinusoidal temperature and mechanical load (a/h=10, MP1)

presented in Fig. 4.17. It is observed from the results that the mesh size of 10 is sufficient for the predicting the non-dimensional deflection accurately. The mesh size of 10 depicts that both the plate is discredited by (10X10) elements.

Further, the considered plate subjected to combined sinusoidal thermal and sinusoidal mechanical load. The thermal load is linearly varying across the thickness (T_1=T_3=0). The effect of boundary conditions (SSSS, SCSS, SCSC and CCCC) and mesh size on non-dimensional deflection is presented in Fig. 4.18.

The non- dimensional deflection parameter $\overline{w}$ is evaluated using the relations defined in Eq. (4.1).It is observed that the mesh size of 10 is adequate for the prediction of the results for this case.

Further in order to ensure the accuracy of the results of the present modal, the results are compared with the closed form solution for simply supported boundary conditions for a four layered anti-symmetric [0^0/90^0/0^0/90^0] square plate. The material properties of each orthotropic layer of the plate is of MP1. The non -dimensional deflection of the considered plate under sinusoidal thermal load (T_1=T_3=0, q=0) and combined sinusoidal thermal and sinusoidal mechanical load(T_1=T_3=0). The thermal load is linearly varying across the thickness. The results for both the cases are compared with closed form solution with varying span to thickness ratio (a/h) in Fig. 4.19.

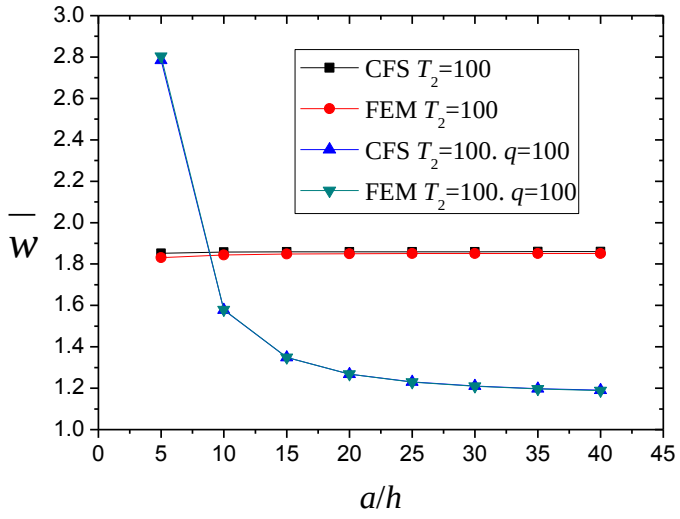

Figure 4.19: Comparison of non-dimensional deflection for simply supported four layered anti-symmetric [0^0/90^0/0^0/90^0] laminated square plate of finite element and closed form solution by varying span to thickness ratio

It is observed that there is a good agreement of results with the closed form solution for various span to thickness ratios.

Further, the considered plate is subjected to uniformly distributed thermal load, in order to investigate the effect of uniform thermal field on non-dimensional deflection. The results are compared with closed form solution (CFS) of various theories for simply supported case (SSSS). The non-dimensional deflection for other boundary conditions (SCSS and SCSC) are presented in Table 4.9. It is observed that the non-dimensional deflection for opposite edges clamped (SCSC) is lesser than that of one edge clamped (SCSS). Moreover, for simply supported case (SSSS), non-dimensional deflection increases with increase in span to thickness ratio, however, non-dimensional deflection decreases with increase in span to thickness ratio for SCSS and SCSC boundary conditions.

Table 4.9: Effect of thickness on dimensionless deflection of anti-symmetric cross ply $[0^0/90^0/0^0/90^0]$ square plate subjected to uniform temperature field

a/*h*	CFS SSSS	FEM SSSS	FEM SCSS	FEM SCSC
5	2.7569	2.7545	2.2037	1.6221
6.25	2.7655	2.7648	2.0994	1.4894
10	2.7848	2.7852	1.8701	1.1784
12.5	2.7926	2.7932	1.7791	1.0455
20	2.8041	2.8047	1.6437	0.8433
25	2.8075	2.8081	1.6062	0.7835
50	2.8125	2.8131	1.5498	0.6951
100	2.8139	2.8146	1.5341	0.6718

Further, the effect of material anisotropy and boundary conditions is investigated on the considered plate under sinusoidal thermal field linearly varying across the thickness. The results for simply supported case (SSSS) are compared with closed form solution Fig. 4.20.

As a later example of this section, simply supported four layered anti-symmetric cross ply $[0^0/90^0/0^0/90^0]$ plate is considered under non-linear thermal field (T_2=T_3=100). The material properties of the plate are taken as MP1. The variation in non-dimensional deflection with thickness of the plate under the sinusoidal (SSL) and uniformly distributed (UDL) linear (T_2=100,T_3=0) and non-linear thermal field (T_2=T_3=100) is presented in Fig. 5.

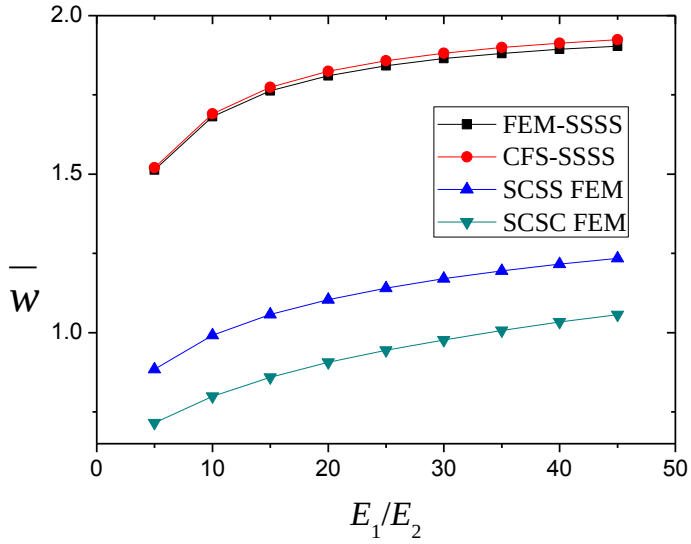

Figure 4.20: Effect of material anisotropy and boundary conditions on the non-dimensional deflection of anti-symmetric cross ply [$0^0/90^0/0^0/90^0$] square plate subjected to sinusoidal temperature field

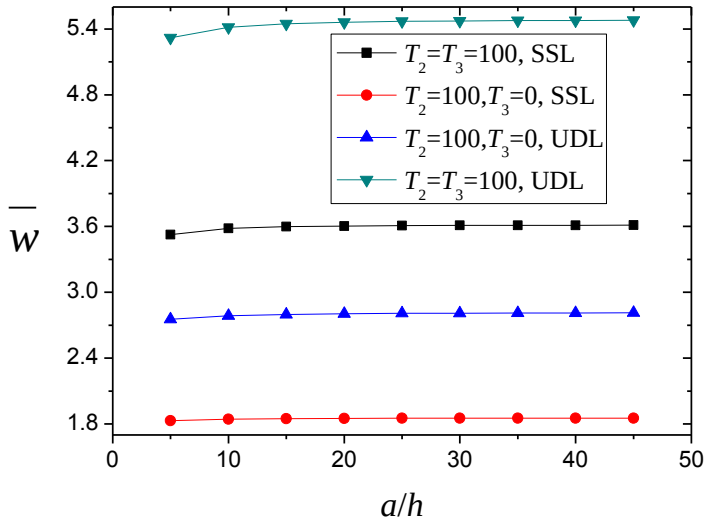

Figure 4.21: Variation in non-dimensional deflection with thickness for four layered anti-symmetric cross ply [$0^0/90^0/0^0/90^0$] plate under various loading conditions

It is observed from the results that there is notable increase in the non-dimensional deflection for the plate under non-linear temperature field as compared to linear temperature field for both SSL and UDL loading.

4.5.2. Thermo-mechanical analysis of symmetric cross-ply plates

The symmetric cross-ply laminates are investigated under various loading and boundary conditions in this section. A three layered symmetric [$0^0/90^0/0^0$] cross ply plate is considered composed of material properties MP1. The plate is first subjected to sinusoidal thermal field linearly varying across the thickness (T_1=T_3=0, q=0). The variation in non-dimensional deflection for different boundary conditions for various values of span to thickness ratio are presented in Table 4.10. The results for simply supported boundary conditions are compared closed form solution with a mesh size of 16. It is observed that the non-dimensional deflection for plate having opposite edges clamped (SCSC) is lesser than that of the plate having one edge clamped (SCSS).

Table 4.10: Effect of boundary conditions on the non-dimensional deflection of three layered symmetric [$0^0/90^0/0^0$] cross ply plate under sinusoidal thermal load.

a/h	SSSS		SCSC	SCSS
	CFS	FEM (16X16)	FEM (16X16)	FEM (16X16)
50	1.0950	1.0629	0.2103	0.2762
10	1.1507	1.1105	0.3501	0.3981
5	1.2517	1.1885	0.5435	0.5721

Further, the considered plate is subjected to combined sinusoidal thermal and transverse loading (T_1=T_3=0). The non-dimensional deflection parameter ($\bar{w}$) is evaluated using the relations defined in Eq. (4.1). The effect of boundary conditions on the non-dimensional deflection for various span to thickness ratios for the considered plate is presented in Table 4.11.

Table 4.11: Effect of boundary conditions on the non-dimensional deflection of three layered symmetric [$0^0/90^0/0^0$] cross ply plate under sinusoidal thermal and transverse load.

a/h	SSSS		SCSS	SCSC	CCCC
	CFS	FEM (18X18)	FEM(18X18)	FEM(18X18)	FEM(18X18)
100	0.9976	0.9970	0.4678	0.2486	0.2470
10	1.6845	1.6015	1.2099	0.9426	0.8602
5	3.4075	3.2868	3.0826	2.7821	2.4105

The results of present finite element modal are compared with the closed form solution for simply supported case. A close agreement between the closed form solution and finite element results is observed. The relative decrement in the non-dimensional deflection by increase in number of clamped sides is lower for thick plates (a/h=5,10) as compared to thin plates (a/h=100).

Further the considered three layered symmetric [$0^0/90^0/0^0$] cross-ply plate is considered under uniformly distributed thermal load. The effect of boundary conditions on the non-dimensional deflection with varying span to thickness ratios for the considered plate is presented in Fig. 4.22. The results are compared with closed form solution of various theories for simply supported case (SSSS). It is observed that the non-dimensional deflection for opposite edges clamped (SCSC) is lesser than that of one edge clamped (SCSS). Moreover, the non-dimensional deflection decreases with increase in span to thickness ratio for SSSS, SCSS and SCSC boundary conditions.

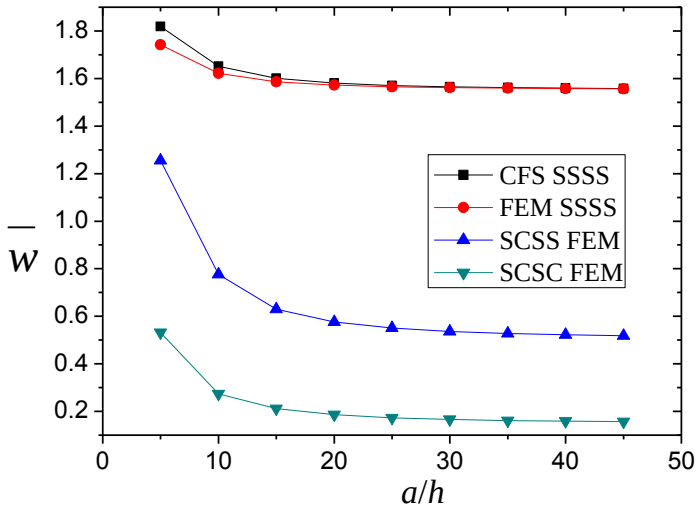

Figure 4.22: Effect of thickness on dimensionless deflection of symmetric cross ply [$0^0/90^0/0^0$] square plate subjected to uniform temperature field

Further, the considered three layered symmetric cross ply [$0^0/90^0/0^0$] plate is considered under non-linear thermal field (T_2=T_3=100). The variation in non-dimensional deflection with thickness of the plate under the sinusoidal (SSL) and uniformly distributed (UDL) linear (T_2=100,T_3=0) and non-linear thermal field (T_2=T_3=100) is presented in Fig. 4.23.

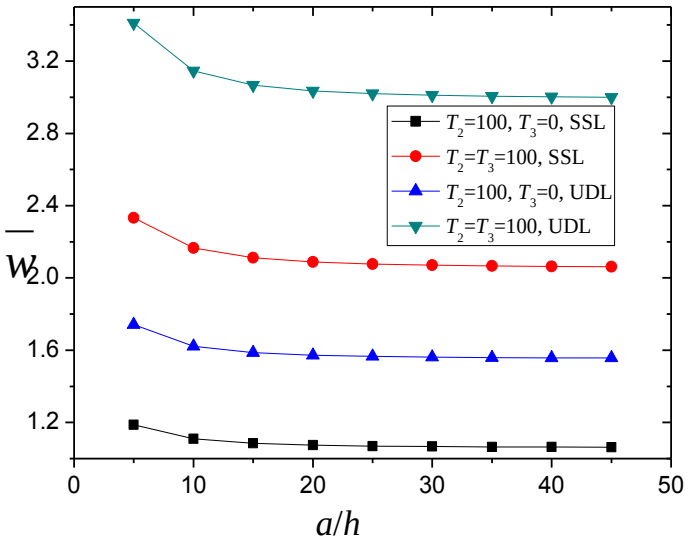

Figure 4.23: Variation in non-dimensional deflection with thickness for three layered symmetric cross ply [0^0/90^0/0^0] plate under various loading conditions

It is observed from the results that there is notable increase in the non-dimensional deflection for the plate under non-linear temperature field as compared to linear temperature field for both SSL and UDL loading.

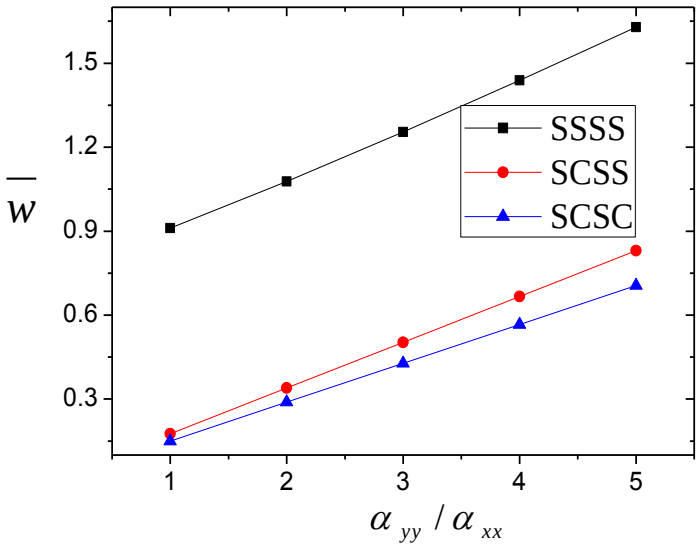

Figure 4.24: Effect of thermal expansion coefficient ratio (α_{yy} / α_{xx}) on non-dimensional deflection for a four layered symmetric [0^0/90^0/90^0/0^0] laminated plate (*a*/*h*=10)

In order to study the effect of thermal expansion coefficient ratio (α_{yy}/α_{xx}) ratio on non-dimensional deflection, a four layered symmetric [$0^0/90^0/90^0/0^0$] laminated plate having material properties of MP1 is considered. The span to thickness ratio of the plate is taken as 10. The results for the considered example are presented in Fig. 4.24. It is observed from the results that the non-dimensional deflection increases linearly with increase in thermal expansion coefficient ratio (α_{yy}/α_{xx}) for the simply supported (SSSS), one edge clamped (SCSS) and opposite edges clamped (SCSC) boundary conditions.

4.5.3. Thermo-mechanical analysis of anti-symmetric angle-ply plates

In order to examine the thermo-mechanical response of anti-symmetric angle-ply plates, a four layered anti-symmetric [$45^0/-45^0/45^0/-45^0$] angle ply plate is considered. The material properties of each layer of the plate are taken as specified in MP2 with simply supported boundary conditions. The plate is first subjected to sinusoidal thermal load and then subjected to combined sinusoidal thermal and sinusoidal mechanical loading. The results for both the cases are presented in Fig. 4.25. The results are validated with the closed for solution. A close agreement of finite element results with the closed form solution is observed.

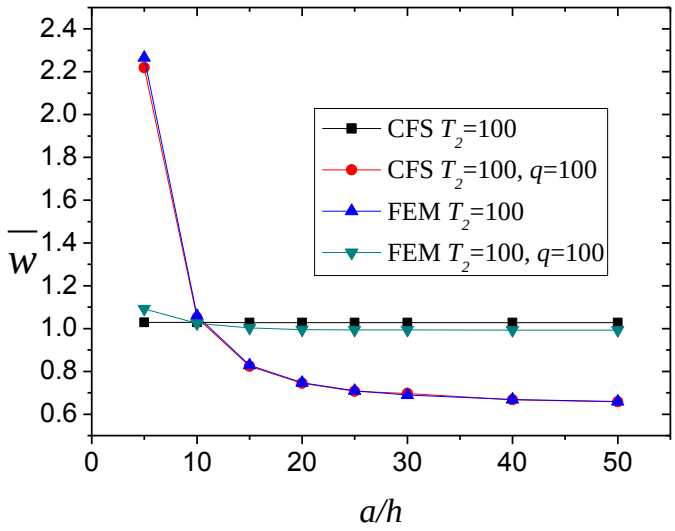

Figure 4.25: Variation in non-dimensional deflection with respect to change in span to thickness ratio for simply supported four layered anti-symmetric [$45^0/-45^0/45^0/-45^0$] angle ply plate under various loading conditions.

Further, the effect of angle of fibre orientation on the dimensionless deflection of four layered $[\Theta/-\Theta]_2$ square anti-symmetric angle-ply plate under sinusoidal thermal load is depicted in Fig. 4.26. The fiber angle is varied from 0^0 to 45^0. The results are compared with the closed form solution for the span to thickness ratio of 10.

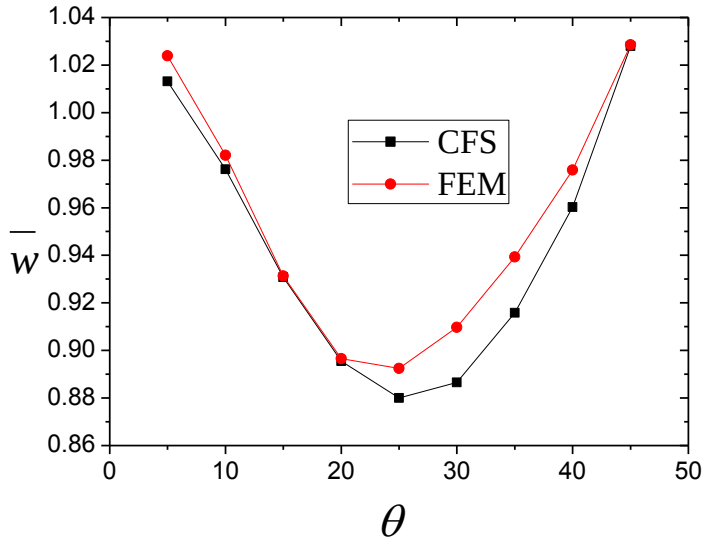

Figure 4.26: The effect of fibre orientation on non-dimensional deflection for four layered anti-symmetric $[\Theta/-\Theta]_2$ angle ply plate subjected to sinusoidal thermal load

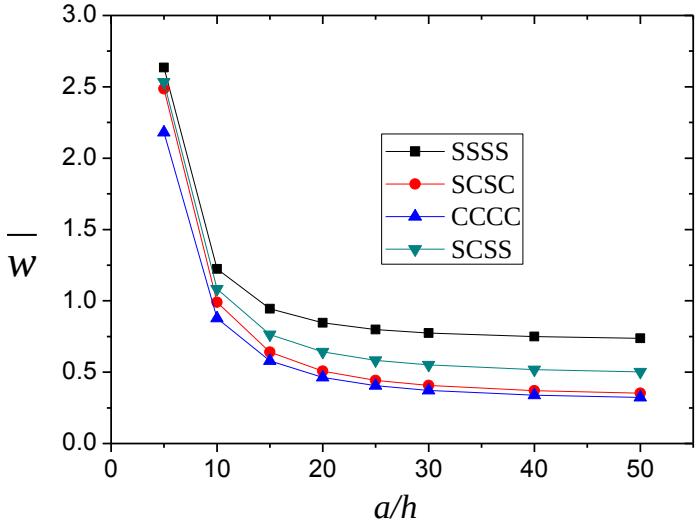

Figure 4.27: Variation in non-dimensional deflection with change in span to thickness ratio for four layered anti-symmetric $[30^0/-30^0/30^0/-30^0]$ angle ply plate subjected to under combined thermal and transverse load

As a later example, four layered anti-symmetric [30^0/-30^0/30^0/-30^0] angle ply plate is considered under combined thermal and transverse load. The material properties of the plate are taken as specified in MP2. The effect of change in span to thickness ratio on non-dimensional deflection for various boundary conditions (SSSS, SCSS, SCSC, CCCC) is presented in Fig. 4.27. It is observed that the relative decrement in non-dimensional deflection for angle ply plates due to increase in number of clamped sides is lesser than that of cross-ply plates.

4.6. Summery

The thermo-mechanical response characteristics of the cross-ply and angle-ply composite plates are examined by implementing analytical and finite element formulation . The IHSDT is implemented to model the laminated composite plates. The validity and applicability of IHSDT is ensured by solving a variety of numerical examples for thermo-mechanical analysis and presenting their comparison with the existing results. The effects of span thickness ratio, material anisotropy ratio, lamination sequence, loading and thermal conditions, aspect ratio and boundary conditions on the thermo-mechanical response characteristics are examined.

CHAPTER-5 CONCLUSIONS AND SCOPE FOR FUTURE WORK

5.1. Conclusions

On the basis of the present research work, the following conclusions are observed which are similar to those observed in the existing literature.

1. The thermo-mechanical response characteristics of the cross-ply and angle-ply composite plates are examined by presenting the closed form solution. The IHSDT is implemented to model the laminated composite plates.

2. The increase in span-thickness ratio decreases the non-dimensional maximum transverse deflection irrespective of the mechanical loading, thermal loading, lamination sequence, and aspect ratio.

3. The analysis of two layered and six layered anti-symmetric angle-ply plate with variable fiber orientation angle (0^0 to 45^0) indicates that the non-dimensional transverse deflection decreases continuously for six layered plate for pure mechanical load and combined mechanical and thermal load. However, for the two layered plate, it increases upto fiber orientation angle of 25^0 and decreases beyond that.

4. The difference in the non-dimensional transverse deflection reduces for the increment in number of layers for any particular lamination sequence.

5. The increment in material anisotropy (E_1/E_2) increases the non-dimensional deflection for symmetric cross ply plates subjected to pure thermal load. However, it reduces the non-dimensional deflection for anti-symmetric angle-ply plates subjected to pure mechanical load.

Following publications are communicated on the basis of present thesis:

1. Joshan YS, Grover N, Singh BN. Analytical Modelling for Thermo-mechanical analysis of Cross-ply and Angle-ply laminated composite plates. Aerospace Science and Technology (Sent for Re-review).

2. Joshan YS, Grover N, Singh BN. Assessment of non-polynomial shear deformation theories for thermo-mechanical of laminated composite plates. Steel and Composite Structures (Under Review)
3. Joshan YS, Grover N, Singh BN. Finite element Modelling for Thermo-mechanical analysis of laminated composite plates. Finite Element in Analysis and Design (Under preparation)
4. Joshan YS, Soni A, Grover N. Thermo-mechanical analysis of anti-symmetric angle-ply laminated plates using secant function based shear deformation theory. Proceedings on 3rd Indian national conference on Applied Mechanics 2017 MNNIT, Allahabad:1:11-12.
5. Joshan YS, Sharma LK, Grover N. Influence of micromechanical properties on thermo-mechanical response of laminated composite plates. International conference on theratical, aplied and theoratical mechanics-2017 IIT, Kharaghpur. (Accepted)

5.2. Scope for future work

1. The influence of temperature on material properties of laminated composite plates may be analysed.
2. The non-linear finite element analysis of thermo-mechanical response characteristics of multi-layered composite plates.
3. Effect of micromechanical properties on non-linear analysis of laminated composite plates under thermo-mechanical loading.

REFERENCES

Aydogdu M. A new shear deformation theory for laminated composite plates. Compos Struct 2009;89:94–101.

Bhaskar K, Varadan TK, Ali JSM. Thermo-elastic solution for orthotropic and anisotropic composite laminates. Compos Part B 1996;27B:415–20.

Carrera E. Theories and finite elements for multilayered, anisotropic, composite plates and shells. Arch Comput Meth Eng 2002;9(2):87–140.

Cetkovic M. Thermo-mechanical bending of laminated composite and sandwich plates using layerwise displacement model. Compos Struct 2015;125:388-99

Chandrashekhara K. Thermal buckling of laminated plates using a shear flexible finite element. Finite Elem Anal Des 1992;12:51–61.

Fares ME, Zenkour AM. Mixed variational formula for the thermal bending of laminated plates. J Therm Stresses 1999;22: 347–65.

Grover N, Maiti DK, Singh BN. A new inverse hyperbolic shear deformation theory for static and buckling analysis of laminated composite and sandwich plates. Compos Struct 2013:95; 667-675.

Kant T, Pandya BN. A simple finite element formulation of a higher order theory for unsymetrically laminated composite plates. Compos Struct 1988;9:215–46.

Khare RK, Kant T, Garg AK. Closed-form thermo-mechanical solutions of higher-order theories of cross-ply laminated shallow shells. Compos Struct 2003;59:313–4

Khdeir AA, Reddy JN. Thermal stresses and deflections of crossply laminated plates using refined plate theories. J Therm Stresses 1991;14:419–38.

Koiter WT. Theory of thin elastic shells. Proceedings of First IUTAM Symposium, Delft North Holland;1950.

Love AEH. The mathematical theory of elasticity, 4th edition. Cambridge University Press, Cambridge;1927.

Maiti DK, Sinha PK. Bending, free vibration and impact response of thick laminated composite plates. Compos Struct 1994;49:115–29.

Mantari JL, Oktem AS, Soares CG. Static and dynamic analysis of laminated composite and sandwich plates and shells by using a new higher-order shear deformation theory. Compos Struct 2011;94:37–49.

Mechab B, Mechab I, Benaissa S. Analysis of thick orthotropic laminated composite plates based on higher order shear deformation theory by the new function under thermo-mechanical loading. Compos Part B Eng 2012;43(3):1453–8.

Meiche NE, Tounsi A, Zlane N, Mechab I, Bedia EAA. A new hyperbolic shear deformation theory for buckling and vibration of functionally graded sandwich plate. Int J Mech Sci 2011;53:237–47.

Mindlin RD. Influence of rotary inertia and shear on flexural motions of isotropic elastic plates. J App Mech 1951;18:31–8.

Reddy JN, Hsu YS. Effects of shear deformation and anisotropy on the thermal bending of layered composite plates. J Therm Stresses 1980;3:475–93.

Reddy JN. A simple higher order shear deformation theory for laminated composite plates. J Appl Mech 1984;51:752–4.

Reddy JN. Mechanics of laminated composite plates. CRC Press; 1999.

Reissner E. The effect of transverse shear deformation on the bending of elastic plates. J App Mech 1945 ;12(2):69–77.

Reissner E, Stavsky Y. Bending and stretching of certain type of heterogeneous elastic plates. J Appl Mech 1951;9: 402-08.

Swaminathan K, Patil SS. Higher order refined computationalmodelwith12 degrees of freedom for the stress analysis of antisymmetric angle-ply plates— analytical solutions. Compos Struct 2007;80:595–608.

Swaminatahan K, Ragounadin D. Analytical solutions using a higher-order refined theory for the static analysis of antisymmetric angle-ply composite and sandwich plates. Compos Struct 2004;64:405-417.

Thai CH , Ferreira AJM, Bordas SPA, Rabczuk T, Xuan HN. Isogeometric analysis of laminated composite and sandwich plates using a new inverse trigonometric shear deformation theory. Eur J Mech A/Solids 2015:43:89-108.

Wu CH, Tauchert TR. Thermoelastic analysis of laminated plates.2: antisymetric cross-ply and angle-ply laminates. J Therm Stresses 1980;3:365–78.

Zenkour AM. Analytical solution for bending of cross-ply laminated plates under thermo-mechanical loading. Compos Struct 2004;65:367–79.

Elements of resultant stiffness matrix $\left[\overline{R^C}\right]$ and force vector $\left\{\overline{F^C}\right\}$:

$$\overline{R_{11}^C} = A_{11}\alpha^2 + A_{66}\beta^2$$
$$\overline{R_{12}^C} = (A_{12} + A_{66})\alpha\beta$$
$$\overline{R_{13}^C} = -(B_{11}\alpha^2 + B_{12}\beta^2 + 2B_{66}\alpha\beta$$
$$\overline{R_{14}^C} = ((\Omega B_{11} + E_{11})\alpha^2 + (\Omega B_{66} + E_{66})\beta^2)$$
$$\overline{R_{15}^C} = (\Omega B_{12} + E_{12} + \Omega B_{66} + E_{66})\alpha\beta$$
$$\overline{R_{22}^C} = A_{66}\alpha^2 + A_{22}\beta^2$$
$$\overline{R_{23}^C} = -(B_{22}\beta^2 + B_{12}\alpha^2 + 2B_{66}\alpha^2)\beta$$
$$\overline{R_{24}^C} = (\Omega(B_{66} + B_{12}) + E_{66} + E_{12})\alpha\beta$$
$$\overline{R_{25}^C} = (\Omega B_{66} + E_{66})\alpha^2 + (\Omega B_{22} + E_{22})\beta^2$$
$$\overline{R_{33}^C} = D_{11}\alpha^4 + (2D_{12} + 4D_{66})\alpha^2\beta^2 + D_{22}\beta^4$$
$$\overline{R_{34}^C} = -((\Omega D_{11} + F_{11})\alpha^2 + (\Omega D_{12} + F_{12})\beta^2 + 2(\Omega D_{66} + F_{66})\beta^2)\alpha$$
$$\overline{R_{35}^C} = -((\Omega D_{12} + F_{12})\alpha^2 + (\Omega D_{22} + F_{22})\beta^2 + 2(\Omega D_{66} + F_{66})\alpha^2)\beta$$
$$\overline{R_{44}^C} = \Omega(\Omega D_{11} + F_{11})\alpha^2 + (\Omega F_{11} + H_{11})\alpha^2 + \Omega(\Omega D_{66} + F_{66})\beta^2 + (\Omega F_{66} + H_{66})\beta^2 + \Omega^2 A_{55} + 2\Omega K_{55} + L_{55}$$
$$\overline{R_{45}^C} = (\Omega(\Omega D_{12} + F_{12}) + (\Omega F_{12} + H_{12}) + \Omega(\Omega D_{66} + F_{66}) + (\Omega F_{66} + H_{66}))\alpha\beta$$
$$\overline{R_{55}^C} = \Omega(\Omega D_{22} + F_{22})\beta^2 + (\Omega F_{22} + H_{22})\beta^2 + \Omega(\Omega D_{66} + F_{66})\alpha^2 + (\Omega F_{66} + H_{66})\alpha^2 + \Omega^2 A_{44} + 2\Omega K_{44} + L_{44}$$

$$\overline{F_1^C} = \alpha\left(A_1^T\overline{T_1} + B_1^T\overline{T_2} + B_1^{AT}\overline{T_3} + \Omega B_1^T\overline{T_3} \right)$$
$$\overline{F_2^C} = \beta\left(A_2^T\overline{T_1} + B_2^T\overline{T_2} + B_2^{AT}\overline{T_3} + \Omega B_2^T\overline{T_3} \right)$$
$$\overline{F_3^C} = -q - \alpha^2\left(B_1^T\overline{T_1} + D_1^T\overline{T_2} + D_1^{AT}\overline{T_3} + \Omega D_1^T\overline{T_3} \right) - \beta^2\left(B_2^T\overline{T_1} + D_2^T\overline{T_2} + D_2^{AT}\overline{T_3} + \Omega D_2^T\overline{T_3} \right)$$
$$\overline{F_4^C} = \alpha\left(\left(\Omega B_1^T + B_1^{AT}\right)\overline{T_1} + \left(\Omega D_1^T + D_1^{AT}\right)\overline{T_2} + \left(\Omega D_1^{AT} + F_1^{AT}\right)\overline{T_3} + \Omega\left(\Omega D_1^T + D_1^{AT}\right)\overline{T_3} \right)$$
$$\overline{F_5^C} = \beta\left(\left(\Omega B_2^T + B_2^{AT}\right)\overline{T_1} + \left(\Omega D_2^T + D_2^{AT}\right)\overline{T_2} + \left(\Omega D_2^{AT} + F_2^{AT}\right)\overline{T_3} + \Omega\left(\Omega D_2^T + D_2^{AT}\right)\overline{T_3} \right)$$